

國立臺灣大學醫學院生理學研究所



碩士論文

Graduate Institute of Physiology

College of Medicine

National Taiwan University

Master Thesis

巨噬細胞在腹膜纖維化中的角色

Macrophage in peritoneal fibrosis

林紀均

Chi-Chun Lin

指導教授：林水龍 博士

Advisor: Shuei-Liong Lin, M.D. Ph.D.

中華民國 106 年 1 月

January, 2017



(附件 2)

國立臺灣大學 (碩) 博士學位論文
口試委員會審定書

巨噬細胞在腹膜纖維化中的角色

Macrophage in peritoneal fibrosis

本論文係林紀均君 (R03441007) 在國立臺灣大學生理所完成之
碩 (博) 士學位論文, 於民國 106 年 01 月 17 日承下列考試委員審查
通過及口試及格, 特此證明

口試委員:

林紀均

(簽名)

(指導教授)

姜文智

吳明仁

系主任、所長

楊志永 (簽名)

(是否須簽章依各院系所規定)

(附件 3)

中文摘要



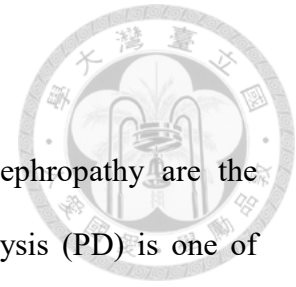
末期腎病的起因大多來自於糖尿性腎病變、腎絲球腎炎和高血壓性腎病變所引起。末期腎病的病人需要進行透析或腎臟移植等治療以取代其喪失的腎臟功能並維持健康，腹膜透析是其中的一個選擇。比起血液透析，腹膜透析有許多優點，包含早期存活率較高、可自行在家操作、費用較低…等，因此吸引許多病人選擇這種治療。然而長時間的腹膜透析仍會造成許多問題的產生，其中最嚴重的問題為腹膜纖維化的形成，使得病人沒辦法繼續進行透析而必須採取其他治療方法。因此，預防及減緩腹膜纖維化成為臨床上必須解決的問題。在我們先前的研究中發現，在腹膜纖維化的過程中，間皮下纖維母細胞 (submesothelial fibroblast) 是肌纖維母細胞的主要來源，並非來自骨髓的纖維細胞或間皮細胞。然而在這過程中巨噬細胞所扮演的角色仍尚未被釐清，因此我們想探討不同來源的巨噬細胞在腹膜纖維化的過程中分別扮演什麼角色。

我們利用 *Csf1r-Cre/Esr1^{Tg};Rs26^{stdTomato/+}* 小鼠，其巨噬細胞給予 Tamoxifen 的誘導下可產生紅色螢光，可藉此觀察當腹膜纖維化時，巨噬細胞的數量及位置。在我們的實驗結果中發現，當給予次氯酸鈉的刺激之後，巨噬細胞的數量會顯著的增加並且累積在腹膜中。因為巨噬細胞顯著增加在受傷的腹膜上，我再利用基因技術讓小鼠巨噬細胞可以因為注射白喉毒素而將巨噬細胞去除，發現將巨噬細胞去除時，原本因纖維化而增厚的腹膜厚度不僅減少，連肌纖維母細胞的數量也減少了。此表示巨噬細胞對於間皮下纖維母細胞轉變為肌纖維母細胞的過程有特定的作用。除此之外，我們也發現這些巨噬細胞並不會表現肌纖維母細胞特定因子 (α -smooth muscle actin; α -SMA) 及膠原蛋白 (collagen)，這個結果顯示巨噬細胞在我們的實驗模式中並不會轉變為肌纖維母細胞。為了探討來自循環及組織駐留的巨噬細胞，我們利用連體共生 (parabiosis) 將 *CAG-EGFP^{Tg}* 和 C57BL/6 小鼠縫合，經過四週後會產生微循環，彼此的周邊血液可進行交換，但腹腔中的細胞並不受影響。實驗結果顯示在次氯酸鈉刺激後，在腹腔內會有約 40% 的巨噬細胞來自於循環中，而剩下 60% 則是組織中的巨噬細胞經由刺激之後增生而來。利用連體共生與基因技術去除來自循環或組織駐留的巨噬細胞，並無法釐清究竟來自循環或組織駐留的巨噬細胞對於腹膜纖維化的影響何者較為重要。

總結來說，當腹膜纖維化時，巨噬細胞會堆積在受傷的腹膜中，但不會轉變成為肌纖維母細胞，因此其扮演的角色可能是藉由細胞間的交互作用影響間皮下纖維母細胞轉變為肌纖維母細胞。循環中及組織中的巨噬細胞在腹膜纖維化過程中，其數量的平衡及表型的變化需要進一步研究。

關鍵字:巨噬細胞、肌纖維母細胞、腹膜纖維化、間皮下纖維母細胞、連體共生

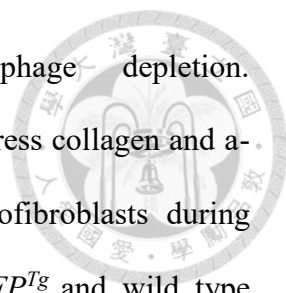
ABSTRACT



Diabetic kidney disease, glomerulonephritis, and hypertensive nephropathy are the leading causes of end-stage renal disease (ESRD). Peritoneal dialysis (PD) is one of therapies for ESRD. PD holds many therapeutic advantages including early survival benefit, the convenience of home therapy, and lower healthcare costs, which are particularly attractive to patients. However, patients will face some challenges especially peritoneal fibrosis after long-term dialysis. Prevention and attenuation of peritoneal fibrosis is an unmet medical need for patients with peritoneal dialysis. In our previous study, we proved that submesothelial fibroblasts are the major origin of myofibroblasts in peritoneal fibrosis. However, the roles of monocytes/macrophages during peritoneal fibrosis are not clear. We tried to figure out the roles of circulating monocyte-derived macrophages and tissue resident macrophages during peritoneal fibrosis in this study.

We used *Csf1r-Cre/Esr1^{Tg};Rs26^{stdTomato/+}* mice whose *Csf1r*-expressing cells including bone-marrow-derived macrophages and yolk sac macrophages expressed red fluorescence protein after tamoxifen-induced genetic recombination. Besides, parabiotic model made by two mice were used to create chimeric mice for study of circulating monocyte-derived macrophages. Sodium hypochlorite was used to induce peritoneal fibrosis.

We first analyzed tissue-resident macrophages in peritoneal cavity and grouped them into two subsets, large peritoneal macrophage (LPM) and small peritoneal macrophage (SPM), as previous studies. After hypochlorite injury, we observed many macrophages accumulated in peritoneum. Selective macrophage ablation in *Csf1r-Cre/Esr1^{Tg};Rs26^{stdTomato/+};Rs26^{iDTR/+}* mice was performed by administration of diphtheria toxin during peritoneal fibrosis. The thickness of injured peritoneum and the number of



myofibroblasts were decreased markedly under macrophage depletion. Immunofluorescence staining showed that macrophages did not express collagen and α -SMA markers, suggesting macrophages did not transit into myofibroblasts during peritoneal fibrosis. In parabiotic model made between *CAG-EGFP^{Tg}* and wild type *C57BL/6* mice, we demonstrated that about 40% of peritoneal macrophages were derived from circulating monocytes and the rest came from tissue-resident macrophages during peritoneal fibrosis. Selective ablation by diphtheria toxin in the parabiotic model made from *Csf1r-Cre/Esr1^{Tg};Rs26^{iDTR/+}* and *Rs26^{iDTR/+}* littermate could not clearly clarify the contribution of circulating monocytes-derived and resident macrophages to peritoneal fibrosis.

In conclusion, our study implicated that macrophages have decisive effects on peritoneal fibrosis but not through macrophage-myofibroblast transition (MMT) pathway. Cross-talk between peritoneal macrophages and submesothelial fibroblasts should be one the underlying mechanisms for the differentiation and scar formation of peritoneal myofibroblasts after injury. The importance of circulating monocyte-derived macrophages and tissue-resident macrophages balance needs further study.

Key word: macrophage, peritoneum fibrosis, myofibroblast, submesothelial fibroblast, parabiosis

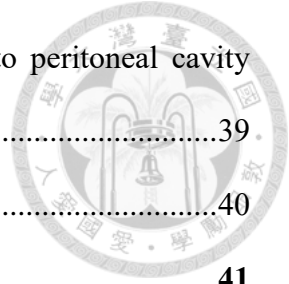
CONTENTS



口試委員會審定書	#
中文摘要	i
ABSTRACT	iii
CONTENTS	v
LIST OF FIGURES	viii
Abbreviations	ix
Chapter 1 Introduction	1
1.1 Physiology of peritoneum	1
1.1.1 Mesothelial cells	1
1.2 Peritoneal dialysis	2
1.3 Peritoneal fibrosis	2
1.3.1 Risk factors	3
1.3.2 The mechanism of peritoneal fibrosis	4
1.4 Animal model of peritoneal dialysis and fibrosis	13
1.4.1 Methods for establishing rodent PD models	13
1.4.2 Peritoneal fibrosis models	14
1.5 Macrophage	15
1.5.1 Origin and functions of tissue macrophages	15
1.5.2 Peritoneal macrophage	16
1.5.3 Macrophage in fibrosis	17
1.5.4 Animal model of conditional macrophage ablation	18
1.6 The purpose of my study	19
Chapter 2 Material and Method	20

2.1	Materials	20
2.1.1	Animals	20
2.1.2	Diphtheria toxin (DT)	23
2.1.3	Chemicals	23
2.1.4	Buffers	26
2.1.5	Antibodies	28
2.1.6	Instruments	31
2.2	Methods	32
2.2.1	Peritoneal fibrosis model.....	32
2.2.2	Chimeric mice model	32
2.2.3	Sample preparation.....	33
2.2.4	Flow cytometry	33
2.2.5	Fluorescence-activated cell sorting (FACS) system.....	34
2.2.6	Immunofluorescence stain	34
2.2.7	Masson's Trichrome stain	35
2.2.8	Isolation of bone marrow cells and measurement of engraftment efficiency	35
2.2.9	Statistical analysis	35
Chapter 3	Results	36
3.1	Identified subsets of macrophages in peritoneal cavity.....	36
3.2	Macrophage increased in injured peritoneum.....	36
3.3	Macrophage ablation by diphtheria toxin	37
3.4	Macrophage ablation attenuated peritoneal fibrosis	37
3.5	Macrophages did not produce collagen and α -SMA in injured peritoneum	38
3.6	Chimeric mice were generated by parabiosis	39

3.7	Circulating monocytes-derived macrophages recruited to peritoneal cavity after injury	39
3.8	Macrophage ablation in parabiosis model	40
Chapter 4	Discussion.....	41
Chapter 5	Conclusion and future prospects	45
REFERENCE		61



LIST OF FIGURES



Figure 1	47
Figure 2	48
Figure 3	50
Figure 4	52
Figure 5	54
Figure 6	56
Figure 7	57
Figure 8	59

Abbreviations



AGEs	Advanced glycation end-products
ANOVA	Analysis of variance
A2A	Adenosine A2a
ADP	Adenosine diphosphate
α SMA	Alpha smooth muscle actin
CCL	Chemokine (C-C motif) ligand
CD	Cluster of differentiation
CG	Chlohexidine gluconate
CKD	Chronic kidney disease
Csflr	Colony stimulating factor 1 receptor
CT	Computer tomography
CTGF	Connective tissue growth factor
C5aR	Complement component 5a receptor
C5L2	Complement component 5a receptor-like 2
DAPI	4', 6-diamidino-2-phenylindole
DMEM	Dullbecco's modified eagle medium
DT	Diphtheria toxin
DTR	Diphtheria toxin receptor
DT-A	Diphtheria toxin fragment A
DT-B	Diphtheria toxin fragment B
ECM	Extracellular matrix
EDTA	Ethelenediaminetetraacetic acid
EGF	Epidermal growth factor

EMT	Epithelial-mesenchymal transition
EPS	Encapsulating peritoneal sclerosis
ESRD	End-stage renal disease
EF2	Elongation factor 2
FACS	Fluorescence-activated cell sorting
FBS	Fetal bovine serum
Fc γ	Fragment crystallizable region γ
FoxP	Forkhead box P
GATA6	GATA-binding factor 6
GDPs	Glucose degradation products
GFP	Green fluorescent protein
HA	Hyaluronic acid
HBEGFR	Heparin-binding epithelial growth factor receptor
HD	Hemodialysis
HGF	Hepatocyte growth factor
HRQoL	Health-related quality of life
ICAM-1	Intercellular cell adhesion molecule-1
IFN- γ	Interferon- γ
IFNGR1	Interferon gamma receptor 1
IGF-1	Insulin-like growth factor 1
IL	Interleukin
IKK	I κ B kinase
IP	Inducible protein
KDOQI	Kidney Disease Outcomes Quality Initiative



KGF	Keratinocyte growth factor
KO	Knock out
LCs	Langerhans cells
LP	Lamina propria
LPA	Lysophosphatidic acid
LMW	Low molecular weight
LPM	Large peritoneal macrophage
LysM	Lysozyme
MAPK	Mitogen-activated protein kinase
MCs	Mesothelial cells
MGO	Methylglyoxal
MRI	Magnetic Resonance Imaging
MCP-1	Monocyte chemoattractant protein-1
MMP	Matrix metalloproteinase
MMT	Macrophage-myofibroblast transition
MHCII	Major histocompatibility complex class II
Mrc-1	Mannose receptor C-type 1
NGS	Normal goat serum
NO	Nitric oxide
PAI-1	Plasminogen activator inhibitor type 1
PAS	Periodic acid-Schiff
PB	Phosphate buffer
PBS	Phosphate buffered saline
PCR	Polymerase chain reaction



PD	Peritoneal dialysis
PDF	Peritoneal dialysis fluid
PD-L2	Programmed cell death protein 1 ligand 2
PDGF	Platelet-derived growth factor
PDGFR	Platelet-derived growth factor receptor
PFA	Paraformaldehyde
PLP	Periodate-lysine-paraformaldehyde
PMSGs	Peritoneal macrophage-specific genes
PPAR	Peroxisome proliferator-activated receptor
PSTR	Peritoneal small solute transport rate
RA	Retinoic acid
RER	Rough endoplasmic reticulum
RFP	Red fluorescent protein
ROR γ t	Retinoic acid receptor-related orphan receptor γ t
ROS	Reactive oxygen species
SDS	Sodium dodecyl sulfate
SES	Supernatant of <i>Staphylococcus epidermidis</i>
Stat	Signal transducer and activator of transcription
SPM	Small peritoneal macrophage
tdTomato	Tandem dimer Tomato
TGF β 1	Transforming growth factor β 1
T _H 1 / 2/ 17	T helper cells type 1 / 2/ 17
TLR	Toll-likel receptor
TNF- α	Tumor necrosis factor- α



Treg	T regulatory cell
tPA	Tissue plasminogen activator
UF	Ultrafiltration
uPA	Urokinase-type plasminogen activator
VCAM-1	Vascular cell adhesion molecule-1
VEGF	Vascular endothelial growth factor



Chapter 1 Introduction



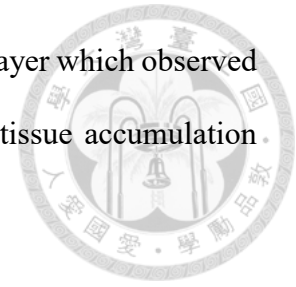
1.1 Physiology of peritoneum

Peritoneum is the thin serous membrane that lines the walls of the abdominal and pelvic cavities. It is the largest serous membrane of human body compare to pericardium and pleura. The peritoneum is lined by a monolayer of mesothelial cells (MCs) which rest on a thin basement membrane supported by connective tissue, fibroblast-like cells, and blood and lymphatic vessels[1]. In physiological conditions, the difference in oncotic pressure across the peritoneal membrane (high at the endothelial layer and low at the mesothelial layer) limits capillary fluid filtration and prevents edema owing to water reabsorption into the capillaries from the interstitial space[2]. As a consequence, peritoneal membrane can serve as a semipermeable membrane for diffuse and filtration in dialysis.

1.1.1 Mesothelial cells

The mesothelium is composed of an extensive monolayer of specialized cells (MCs) that line the body's serous cavities and internal organs, playing important roles in maintaining normal serosal integrity and function[3]. Traditionally, mesothelium contributes two main functions which are to provide a protective barrier and a frictionless interface for the free movement of opposing organs and tissues[3]. As time passed by, it has been discovered that this tissue also plays important roles in fluid and cell transport[4], initiation and resolution of inflammation[5, 6], tissue repair, lysis of fibrin deposits preventing adhesion formation and protection against invading microorganisms and, possibly, tumor

dissemination[7, 8] The disappearance of the mesothelium layer which observed in injured peritoneal membrane might lead to connective tissue accumulation and fibrosis formation[9, 10].

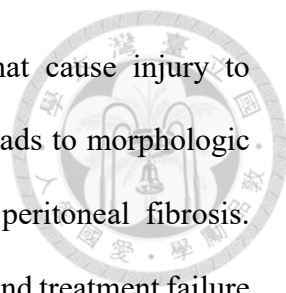


1.2 Peritoneal dialysis

The number of patients treated for terminal kidney failure worldwide has continued to grow up since the beginning of maintenance therapy for end-stage renal disease (ESRD) through dialysis or transplantation[11]. Among causes of ESRD the prevalent causes are the following: diabetic nephropathy, glomerulonephritis, and hypertensive nephropathy[12]. Both hemodialysis (HD) and peritoneal dialysis (PD) are used to treat ESRD patients. HD uses a man-made membrane (dialyzer) to filter wastes and remove extra fluid from the blood. PD uses the PD fluid (PDF) to remove wastes and extra fluid across the peritoneal membrane from the body. About 200,000 ESRD patients around the world rely on the peritoneal membrane to provide dialysis therapy[11]. PD holds extensive therapeutic advantages for appropriately selected patients when compared with HD, including early survival benefit, the convenience of home therapy, and lower healthcare costs, which are particularly attractive to patients[13]. Moreover, some studies demonstrated that PD patients tend to have better preservation of residual renal function and higher health-related quality of life (HRQoL) than HD patients[12, 14].

1.3 Peritoneal fibrosis

After long-term dialysis, patients may face some challenges. Bio-incompatible



PDF, uremia, and peritonitis are the common reasons that cause injury to peritoneal membrane[15]. Injury to peritoneal membrane leads to morphologic and functional changes, and increases the possibility of peritoneal fibrosis. Peritoneal fibrosis is a major factor leading to ultrafiltration and treatment failure in the patients on PD therapy[16]. Classically, peritoneal fibrosis can be grouped into two types. Type I is simple peritoneal fibrosis and Type II is encapsulating peritoneal sclerosis (EPS)[17, 18]. The peritoneum could repair itself from the type I simple peritoneal fibrosis which is composed of mild inflammation and related to vintage on PD. Unlike type I peritoneal fibrosis, the EPS, type II peritoneal fibrosis, is the most severe form and can increase mortality rate to exceed 50% as a result of complications related to malnutrition, persistent bowel obstruction, bowel perforation, prolonged parenteral feeding and infection[19].

1.3.1 Risk factors

Many factors can contribute to PD-related tissue remodeling, including uremia, peritonitis, the presence of the catheter, and instillation of the bio-incompatible PDF itself. The interaction between these factors complicatedly could be the reasons of peritoneal fibrosis[20]. In 2008, a Japanese research group found that uremia and diabetes had an impact on the pathogenesis of peritoneal sclerosis in pre-PD peritoneum[21]. However, the leading cause of peritoneal fibrosis has been considered to be the PDF which is bio-incompatible due to high osmolarity, low pH, high glucose concentration, advanced glycation end product (AGEs), and glucose degradation product (GDP). The bio-incompatible PDF is believed to trigger an injury-repair process which consists of a low-grade chronic

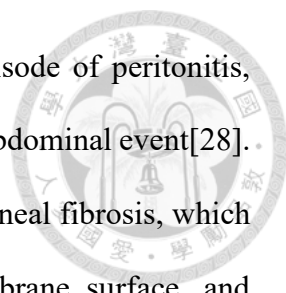
inflammation, loss of MCs, accumulation of myofibroblasts, micro-vascular degeneration and neo-angiogenesis[21, 22].

High glucose concentration has shown to damage peritoneal MCs by increasing growth factors and matrix proteins[20, 23]. GDP, particularly 3-deoxyglucosone (3-DG) and methylglyoxal (MGO), have been proved to accelerate AGE formation more potentially than glucose itself[24]. The deposition of AGE in the peritoneal membrane correlates with the development of peritoneal fibrosis and loss of ultrafiltration[25] possibly by stimulating production of extracellular matrix (ECM) and changing the peritoneal microvasculature through synthesis of growth factors, such as transforming growth factor- β 1 (TGF- β 1) and vascular endothelial cell growth factor (VEGF)[18, 26].

Recurrent peritonitis, the severity of infection and the number of episodes encountered are strongly associated with peritoneal fibrosis. Many studies demonstrate that inflammation drives fibrosis in a wide variety of pathologies, and animal models of PD suggest that interleukin 6 (IL-6) signaling in recurrent inflammation is the key mechanism[16]. Most common bacterial infections in PD peritonitis are caused by *Staphylococcus epidermidis* and *Escherichia coli*.

1.3.2 The mechanism of peritoneal fibrosis

Although type I peritoneal fibrosis is shown in almost every ESRD patient on PD for a period, the pathogenesis of type II peritoneal fibrosis, or the most disastrous EPS, however, still remains uncertain. A widely accepted hypothesis for EPS is the “two-hit theory”[27]. The first hit has been proposed to be the disruption of normal peritoneal/mesothelial physiology as a consequence of long



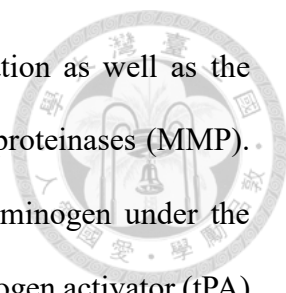
standing PD. The second hit may take the form of an episode of peritonitis, genetic predisposition, discontinuing PD, or an acute intra-abdominal event[28]. The second hit is thought to play a key role of type II peritoneal fibrosis, which the peritoneum could produce heavy adherence of membrane surface, and increase TNF and IL-6 expression in this condition leading to EPS.

1.3.2.1 The pathological change in peritoneal fibrosis

Simple sclerosis or fibrosis is the most common peritoneal pathology of long-term PD whereas EPS is very rare. The thickening of peritoneum in the absence of encapsulation can be observed in simple sclerosis. EPS tissue is characterized by mesothelial denudation, thickening of sub-mesothelial compact zone, hyalinization and sclerosis of the peritoneal vasculature (vasculopathy), neoangiogenesis as well as interstitial fibrosis[28]. In addition, inflammatory cells infiltration, fibrin deposition, even AGEs are found to be present in the mesothelial and sub-mesothelial layer of PD patients[29, 30].

1.3.2.2 Inappropriate balance between fibrin deposition and breakdown

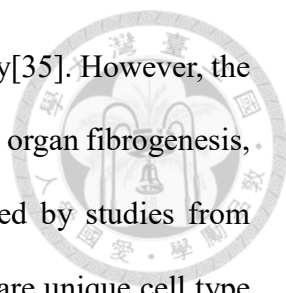
Peritoneal inflammation increases the production of fibrin exudation which can either be lysed or remodeled by invading fibroblasts leading to fibrosis and adhesion formation. The unbalanced ratio between procoagulant and anticoagulant factors causes accumulation of the ECM, which are responsible for the peritoneal fibrosis[31]. Plasmin



(anticoagulant) plays a key role in fibrin degradation as well as the turnover of ECM and activation of matrix metalloproteinases (MMP). Plasmin is made from the inactive zymogen plasminogen under the influence of plasminogen activators: tissue plasminogen activator (tPA) and urokinase-like plasminogen activator (uPA). Whereas, plasminogen activation inhibitors (PAI-1 and PAI-2) can inhibit the activation of plasminogen. Besides endothelium and placenta, MCs express PAI-1 and PAI-2 after TGF- β activation[32]. Previous study findings that low levels of plasmin and high levels of PAI were measured of patients on PD compared with HD patients suggested a higher degree of hypercoagulation in patients on PD therapy[33]. These evidence demonstrated that such an inappropriate balance between fibrin deposition and breakdown increases the probability of fibrous adhesion formation possibly contributing to the development of peritoneal fibrosis[28].

1.3.2.3 Scar-producing myofibroblasts during peritoneal fibrosis

Epithelial mesenchymal transition (EMT) is a complicated process involved in a variety of normal physiologic processes, including gastrulation, heart formation, and palate closure during embryogenesis[34]. This complex process is tightly regulated and requires the correct spatiotemporal expression, interaction and modification of a multitude of intra-and extracellular factors to allow a change in cell phenotype. EMT is also involved in many pathologic



processes such as metastatic potential in malignancy[35]. However, the prevalent hypothesis for the involvement of EMT in organ fibrogenesis, including renal fibrosis[36-40] has been overturned by studies from independent groups including ourselves[10]. MCs are unique cell type which express both epithelial and mesenchymal markers under normal condition. Many studies demonstrated MCs start to lose cell-cell contact and apical-basal cell polarity and invade the basal lamina changing to a mesenchymal phenotype expressing α -smooth muscle actin, depositing ECM and thickening the peritoneal membrane when exposed to injurious agents[41].

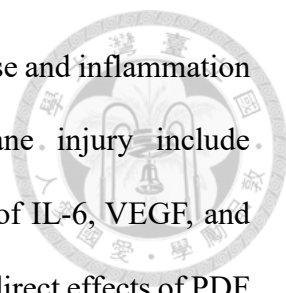
In terms of peritoneal fibrosis, abundant evidence points to MCs as being the principal source of myofibroblasts via a process of EMT[18]. In 2003, Yáñez-Mo et al. found that peritoneal MCs undergo a transition from an epithelial phenotype to a mesenchymal phenotype[39]. Peritoneal MCs isolated from clinical patients' dialysis fluid effluents displayed a mesenchymal phenotype and showed a decrease in the expression of cytokeratin and E-cadherin. Another group, Yang et al., demonstrated that TGF- β 1 induced human omental MCs to transdifferentiate into myofibroblasts in vitro with the characteristic appearance of prominent rough endoplasmic reticulum (RER), conspicuous smooth muscle actin myofilaments, intermediate and gap junctions and active deposition of ECM[38]. TGF- β 1 is pointed to be a principal mediator of mesothelial EMT as demonstrated both in vitro[38, 42] and in vivo[40]. Although previous evidence proved that

mesothelial EMT exists in the development of peritoneal fibrosis, how much an important role it plays in the fibrotic process is a matter of debate.

Our previous study used tamoxifen-inducible Cre/Lox techniques to genetically label and fate map MCs and submesothelial (SM) fibroblasts. To determine whether SM fibroblasts were the primary source of α SMA⁺ myofibroblasts, we generated *Colla2-CreERT^{Tg};ROSA26^{fsdTomato};Colla1-GFP^{Tg}* mice in which cells expressing the Colla2 chain of collagen I could undergo somatic recombination to express the tdTomato RFP permanently after tamoxifen administration (Colla2-RFP⁺ cells). Two weeks after cohort labeling, hypochlorite injury was induced. After 1 week, the numbers of Colla2-RFP⁺ cells and Colla1-GFP⁺ cells increased; the proportion of Colla1-GFP⁺ cells that coexpressed Colla2-RFP was 63.0%. The absence of a significant decrease in the proportion of Colla1-GFP⁺ cells coexpressing Colla2-RFP indicated that SM fibroblasts, rather than other cell sources, were the major precursors of collagen-producing cells in the injured peritoneum[10].

1.3.2.4 Inflammatory cellular profile

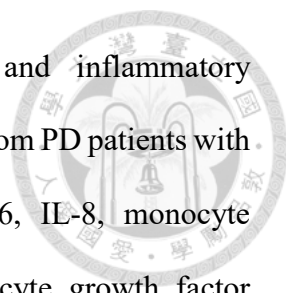
A major factor limiting PD remains peritoneal membrane failure due to peritoneal fibrosis driven by inflammation caused by infections or sterile cellular stress. The bio-incompatible PDF is thought to be the culprit for the sterile inflammation[43-45]. Evidence has showed that



PDF components have an impact on immune defense and inflammation of host peritoneum[45]. Mediators of membrane injury include inflammatory cytokines, notably local production of IL-6, VEGF, and TGF- β [46]. These evidences indicate that not only direct effects of PDF component on membrane structure but also indirect effects related to host defense and exaggerated inflammation contribute to the PDF-induced sterile inflammation[45].

Besides, PD-related inflammation is not only a local event but also an important source leading to systemic inflammation[47-49]. In 2013, Lambie M et al. analyzed the systemic and local inflammation in PD patients[48]. They studied 959 patients and found that local peritoneal and systemic inflammation was uncouple[48]. Systemic inflammation was associated with age and comorbidity and independently predicted patient survival, whereas intraperitoneal inflammation was the most important determinant of peritoneal small solute transport rate (PSTR) but did not affect survival[50]. These evidences indicated that systemic and local intraperitoneal inflammation represent distinct processes and consequences in PD patients. As a consequence, the PD-related inflammation requires different therapeutic approaches which depends on locally or systemically. However, these findings didn't mean that there's no cross talk between local and systemic reactions. Also, the importance of membrane inflammation itself in these process is still unclear.

Many clinical studies have demonstrated that some cytokines are

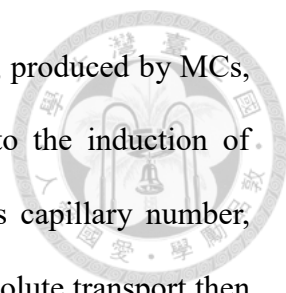


involved in bacterial peritonitis. Leukocytes and inflammatory mediators increase in peritoneal effluent obtained from PD patients with episodes of bacterial peritonitis[51]. IL-1 β , IL-6, IL-8, monocyte chemotactic protein-1 (MCP-1), TGF- β 1, hepatocyte growth factor (HGF), and platelet-derived growth factor (PDGF) are involved in repeating peritonitis and lead to peritoneal fibrosis[51, 52].

Some studies indicate that fibrosis is associated with retention of an activated leukocyte population within the infected organ[16, 53]. Inflammatory cytokines have been linked to the development of fibrosis in autoimmune conditions such as systemic sclerosis or interstitial lung disease[54]. Acute inflammatory response in peritoneum can be evoked by overexpression of IL-1 β and TNF- α which induce an early expression of angiogenic cytokine VEGF and profibrotic cytokine TGF- β 1, along with fibronectin expression and collagen deposition in peritoneal tissue[55].

IL-8 and MCP-1 are found in steady state PD effluents and elevated levels upon peritonitis[56]. Interestingly, hyaluronan (HA) fragments, produced by MCs upon inflammation and wound healing, induce the release of IL-8 and MCP-1[57, 58]. Classically, high molecular weight HA is thought to promote healing of the injured mesothelium by creating a fibrin network and limiting the damaging effects of free radicals[58]. But, in here, the reason that increased level of HA in peritonitis still unclear.

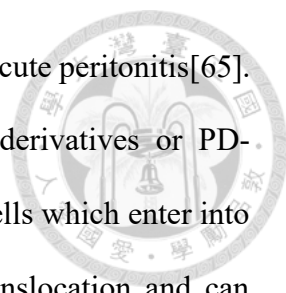
VEGF and TGF- β are thought to be the most important growth factors



contributed to peritoneal tissue remodeling. VEGF, produced by MCs, affects endothelial permeability and contributes to the induction of angiogenesis. Elevating of VEGF levels increases capillary number, and vessel permeability, leading to increase small solute transport then decline of peritoneal function and finally ultrafiltration failure[18, 26]. High glucose concentrations upregulate TGF- β , inducing peritoneal fibrosis[59]. Also, in many animal studies showed that overexpression of TGF- β in the peritoneum caused peritoneal fibrosis, angiogenesis, EMT, increased peritoneal membrane transport, and reduced ultrafiltration[40, 60].

Toll-like receptors (TLRs) are essential to evoke a rapid inflammatory response to infections[45, 61]. TLRs are expressed in various cell types, including peritoneal macrophages and MCs[62], recognize microorganisms and their components. Once TLRs are activated, proinflammatory and fibrotic mediators (e.g., IL-6, TGF- β , TNF- α , and IL-8) will be released to trigger inflammations[16, 63]. Raby AC et al. used knockout mice to reveal that a major role for TLR2, a lesser role for TLR4, a supplementary role for C5aR, and no apparent activity of C5L2 in infection–induced peritoneal fibrosis[64]. Thus, these findings demonstrated the influence of peritoneal TLR2 and TLR4, expressed on peritoneal macrophages and MCs, on PD-associated fibrosis and provide a therapeutic strategy against fibrosis[64].

Besides the innate immunity effects, more recent studies disclose the implication of the Th1, Th17 and Treg roles in fibrotic diseases. Th1



immune response is developed during episodes of acute peritonitis[65]. PD-related factors, including bacteria and their derivatives or PD-catheter or AGEs or IL-6, locally stimulate Th17 cells which enter into the peritoneal cavity through or via intestinal translocation and can provoke peritonitis episodes[66]. Th17 cells may mediate strong inflammation by producing a cocktail of cytokines such as IL-6, IL-17A, IL-17F, and IL-22, among which IL-17A has been defined as the major effector cytokine in causing a sustained inflammatory response[67]. Rodrigues-Díez et al. first found in both mice and human samples that IL-17 is overexpressed in injured peritoneal biopsies[68]. In addition, after repeated intraperitoneal injection of IL-17, mice developed peritoneal fibrosis which was similar to that shown in PD patients[68]. On the contrary, use of IL-17A neutralizing antibody can reduce peritoneal fibrosis in mice exposed to PDF for 35 days[68]. Peroxisome proliferator-activated receptor γ (PPAR- γ) agonists, used to treat type II diabetes, have been found some beneficial effects on inflammation, fibrosis, and angiogenesis[69]. One study demonstrated that rosiglitazone, a PPAR γ agonist, augments the intraperitoneal IL-10 levels (Treg-associated cytokine), increases the recruitment of Treg, and finally attenuates peritoneal fibrosis in an experimental mouse PD model[70]. This study implicated that regulatory T cells play an important role in the protection of the peritoneal membrane.

1.4 Animal model of peritoneal dialysis and fibrosis

Many researchers have been using different animals including rabbits, dogs, pigs, rats, and mice to perform PD-related researches. Rodent is the most convenient and widely used among these animals. More than simple intraperitoneal injection of PDF, the abdominal cavity intubation technique has been increasingly refined and can provide a satisfactory model. Use of animal models of PD and appraisalment of any resulting complications are critical to the study of the pathophysiologic process. Establishment of a standard model is also important in analyzing and adapting the data to the clinic.

1.4.1 Methods for establishing rodent PD models

Intraperitoneal PDF retention through direct injection or implanted catheter are the two common methods for establishing rodent PD models. Ten to 30 mL PDF per injection in the rat and 1.5–2.5 mL PDF per injection in the mouse once daily for up to 20 weeks are usually used. Another method of implanting a catheter into the abdomen of rats or mice involves making a small incision in the middle of the abdominal wall, while the animal is under anesthesia and insertion of a special silicone catheter through the subcutaneous tunnel to the neck or back[71-73]. The animals are then allowed to recover for a week following surgery and given heparinized saline or isotonic saline once each day through the mini-tube to prevent tube blockage and to promote wound healing. Similarly simulating the pathological and physiological processes in patients is a big advantage of the catheter implantation method compare to other methods. However, more difficult surgical procedure, an increased rate of mortality due to the higher risk

of infection and severe local inflammation around the catheter are the shortages of this method.




1.4.2 Peritoneal fibrosis models

The features of peritoneal fibrosis are accumulation of ECM and neoangiogenesis in the submesothelial zone. Administration of PDF for an extended period of time, 5 weeks in rat or 4 weeks in mice can lead to different grades of peritoneal fibrosis[74, 75]. Besides, intraperitoneal injection of a stimulating chemical, typically chlorhexidine gluconate (CG) or sodium hypochlorite (NaOCl), is an easier way to induce peritoneal fibrosis. The last approach is to damage the peritoneum mechanically. The peritoneum may be scraped with tools like the top of a 15-mL centrifuge tube either blindly or in a predetermined direction[76]. We also use infection model to induce repeated peritonitis leading to peritoneal fibrosis. Acute peritoneal inflammation of this model is induced by administration a controlled dose of cell-free supernatant of *Staphylococcus epidermidis* (SES), which is a major cause of PD-associated peritonitis[51]. Four sequential rounds of acute SES-induced peritoneal inflammation was induced at a 5-day interval and fibrosis would develop after repetitive acute inflammation. This mouse model imitates acute human PD peritonitis, with early activation of proinflammatory cytokines (TNF α , IL-1, and IFN- γ) and subsequent changes in chemokine expression and the rapid recruitment of neutrophils and their subsequent replacement by monocytes[51].

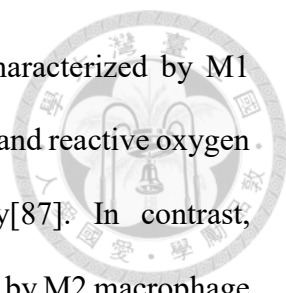
1.5 Macrophage

1.5.1 Origin and functions of tissue macrophages



In the 19th century, macrophages were first discovered by Ilya Metchnikoff and are evolutionary conserved phagocytes that evolved more than 500 million years ago[77]. In 1968, Ralf van Furth, Zanvil Cohn and colleagues formulated the mononuclear phagocyte system: the origin of all macrophages is terminal differentiation from blood monocytes and this hypothesis has prevailed for a long time[78]. This view has dramatically shifted recently with the observation that macrophages from embryonic progenitors can persist into adulthood and self-maintain by local proliferation[79, 80] with minimal input from circulating monocytes. In some cases, tissue-resident mononuclear phagocytes are exclusively embryo-derived, such as microglia in the brain and Langerhans cells (LCs) in the epidermis. Conversely, others tissue resident macrophages are constantly replaced from monocytes, for example intestinal lamina propria (LP) and dermal macrophages[81, 82]. Many tissue-resident macrophages reflect an intermediate situation and can be of mixed origin properly[83]. Resident macrophages can modulate tissue homeostasis via acting as sentinels and responding to changes in physiology as well as challenges from outside.

Macrophages perform important immunological functions during the innate response to microorganisms and the initiation of inflammation but also contribute to the maintenance of tissue homeostasis, tissue regeneration[84] and cancer pathogenesis[85]. Plasticity and flexibility are key features of mononuclear phagocytes and of their activation states[77]. Likely, macrophages have different character in early and later phase of inflammation[86]. Several

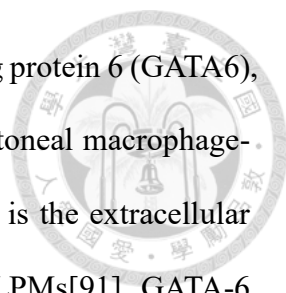


evidences show that initial infiltration of macrophages, characterized by M1 macrophages, culminate with pro-inflammatory cytokines and reactive oxygen species (ROS) production and exacerbate inflammatory[87]. In contrast, macrophage in the later phase of inflammation, characterized by M2 macrophage, has been associated with release of anti-inflammatory molecule and growth factors, which attenuate inflammation and promote tissue regeneration[88].

1.5.2 Peritoneal macrophage

Peritoneal macrophages, one of the best-studied macrophage populations, play important roles in clearing apoptotic cells and coordinating inflammatory responses. Currently, it was demonstrated the co-existence of two subsets in mouse peritoneal cavity, which exhibit developmentally and functionally distinct populations[89]. In the peritoneal cavity, two peritoneal macrophage subsets have been defined: large peritoneal macrophage (LPM) and small peritoneal macrophage (SPM). LPM make up the majority of peritoneal macrophages and express high levels of F4/80 and CD11b, but lack MHC class II (MHCII) while SPM, whereas, express lower levels of F4/80 and CD11b but high levels of MHCII. F4/80^{hi} peritoneal macrophages (LPM) are demonstrated that they can maintain locally by self-renewal throughout adult life and are predominantly independent of hematopoiesis[90]. Conversely, SPM derive from blood monocytes that migrate into the peritoneal cavity in large numbers in response to the stimulation and have tissue half-lives of only a few days[89].

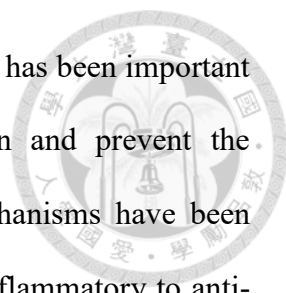
In the last few year, a great advance in the understanding of the transcriptional control of peritoneal macrophages provided novel approach to clarify their



functions. The zinc finger transcription factor GATA-binding protein 6 (GATA6), expressed by LPM, appears to regulate the majority of peritoneal macrophage-specific genes (PMSGs)[91]. Moreover, retinoic acid (RA) is the extracellular factor that regulates GATA-6-specific gene expression in LPMs[91]. GATA-6 not only regulates of gene expression profiling in peritoneal macrophages, also appears to be involved in the control of the proliferation, survival, and metabolism of these cells[92]. Furthermore, Accarias S et al. used single cell-based qPCR coupled with flow cytometry analysis to further define the phenotypes of large and small resident[93]. They found that the expression of Cxcl13, IfngR1, Fizz-1 and Mrc-1 can clearly distinguish between LPMs and SPMs subsets peritoneal macrophages respectively[93].

1.5.3 Macrophage in fibrosis

One of the most interesting features of macrophage function is their involvement in tissue repair and regeneration. Macrophages are activated by endogenous dangers signals and pathogen-associated molecular patterns when they encounter invading organisms or necrotic debris after injury. These activated macrophages produce anti-microbial mediators, including reactive oxygen and nitrogen species and proteinases, that help to scavenge invading pathogens[85]. However, they also produce a variety of inflammatory cytokines and chemokines such as TNF- α , IL-1, IL-6 and CCL2 which evoke inflammatory and anti-microbial responses[94]. This exacerbates tissue injury and leads to aberrant wound healing and fibrosis in some cases if the response is not properly controlled[95]. In many chronic fibrotic diseases, the tissue-damaging irritant is



either unknown or cannot be eliminated easily. Therefore, it has been important to elucidate the mechanisms that suppress inflammation and prevent the development of fibrosis. A variety of mediators and mechanisms have been shown to regulate the macrophage conversion, from pro-inflammatory to anti-inflammatory, including the cytokines IL-4 and IL-13, Fcγ receptor and TLR signaling, the purine nucleoside adenosine and A2A receptor signaling, prostaglandins, Treg cells, and B1 B cells[96, 97]. Another variety of soluble mediators, like IL-10, arginase 1, IKK α , MMP13, maresins, CD200, RELM α and PD-L2, which have all been shown to decrease the magnitude and/or duration of inflammatory responses, and in some cases to contribute to the resolution of fibrosis[98]. Each of these mediators has been demonstrated to activate distinct populations of macrophages with suppressive or regulatory features. As a consequence, current fibrosis studies are focused on characterizing these regulatory macrophage populations and inventing therapeutics strategies that can exploit their anti-inflammatory, anti-fibrotic and wound-healing properties.

1.5.4 Animal model of conditional macrophage ablation

Diphtheria toxin (DT) is secreted from *Corynebacterium diphtheriae* as a secretory single polypeptide. DT binds a toxin receptor which is on the cell surface of toxin-sensitive cells through fragment B (DT-B)[99] and is incorporated into the cells by receptor-mediated endocytosis. Fragment A (DT-A) catalyzes the transfer of ADP-ribose to all eukaryotic EF-2s result in inhibition of protein synthesis and subsequent toxin-sensitive cells death, yet

mice and rats remain insensitive to DT[100]. Since mice are insensitive to DT, this advantage provided an opportunity for a unique ablation strategy[101, 102]. We can use transgenic expression of a diphtheria toxin receptor (DTR) in mouse cells and application of diphtheria toxin (DT) for lineage ablation[103].

1.6 The purpose of my study

The macrophage populations are highly heterogeneous and have different specialized functions. However, the role of macrophages in peritoneal fibrosis is still unclear. The purpose of my study is to clarify the role of macrophages in peritoneal fibrosis.

Chapter 2 Material and Method



2.1 Materials

2.1.1 Animals

2.1.1.1 C57BL/6 mice

Wild-type *C57BL/6* mice were obtained from the Laboratory Animal Center of College of Medicine, National Taiwan University.

2.1.1.2 *Csf1r*-Cre/*Esr1*^{Tg} mice

The transgenic mice express MerCreMer fusion protein under control of the macrophage specific *Csf1r* (colony stimulating factor 1 receptor) promoter after Tamoxifen induction. The transgenic mice are FVB/N background which obtained from The Jackson Laboratory.

2.1.1.3 *C57BL/6*-Gt(ROSA)26^{Sortm1(HBEGF)Awai/J} reporter mice (*Rs26*^{iDTR/iDTR} mice)

The simian *Hbegf* which known as Diphtheria Toxin Receptor was inserted into the Gt(ROSA)26Sor (ROSA26) locus in these mice. When these mice bred to a strain with the Cre recombinase expressing in the specific cells or tissues, these mutant mice strain may be useful in studies of the specific cell ablation following the Diphtheria toxin administration.



2.1.1.4 *Colla1*-GFP transgenic mice

Colla1-GFP^{Tg} were generated and validated as previously described on the C57BL6 background.

2.1.1.5 B6.Cg-Tg(*Gt*(ROSA)26Sor-EGFP)*I1Able*/J (*Rs26-EGFP^{Tg}*)

B6.Cg-Tg(Gt(ROSA)26Sor-EGFP)I1Able/J also known as *Rs26-EGFP^{Tg}*. EGFP in these ROSA26-EGFP BAC transgenic mice is expressed in all tissues and organs examined, which is useful in transplantation studies and cell lineage analyses.

2.1.1.6 C57BL/6-Tg (CAG-EGFP) 10sb/J transgenic mice

C57BL/6-Tg (CAG-EGFP) 10sb/J transgenic mice referred as *CAG-EGFP^{Tg}* (JAX#003291). This transgenic mouse line with an "enhanced" GFP (EGFP) cDNA under the control of a chicken beta-actin promoter and cytomegalovirus enhancer makes all of the tissues, with the exception of erythrocytes and hair, appear green under excitation light.

2.1.1.7 B6.Cg-Gt(ROSA)26Sortm14(CAG-tdTomato)Hze/J mice (*Rs26^{stdTomato/tdtomato}*)

The mutation of the *Gt(ROSA)26Sor* locus with a loxP-flanked STOP cassette prevents the transcription of a CAG promoter-driven red fluorescent protein variant (tdTomato) in these mice. Cells or tissues express tdtomato fluorescence following the Cre-mediated

recombination.



2.1.1.8 *Csflr-Cre/Esr1^{Tg};Rs26^{fstdTomato/+}* mice

We generate *Csflr-Cre/Esr1^{Tg};Rs26^{fstdTomato/+}* mice by cross *Csflr-Cre/Esr1^{Tg}* with *Rs26^{fstdTomato/tdTomato}* mice. After tamoxifen induction, *Csflr* expression cells would have tdtomato fluorescence.

2.1.1.9 *Csflr-Cre/Esr1^{Tg};Rs26^{iDTR/+}* mice

We generate *Csflr-Cre/Esr1^{Tg}; Rs26^{iDTR/+}* mice by cross *Csflr-Cre/Esr1^{Tg}* with *Rs26^{iDTR/iDTR}* mice. After tamoxifen induction, *Csflr* expression cells would have human DT receptor.

2.1.1.10 *Csflr-Cre/Esr1^{Tg};Rs26^{fstdTomato/+};Colla1-GFP^{Tg}* mice

we generated *Csflr-Cre/Esr1^{Tg};Rs26^{fstdTomato/+};Colla1-GFP^{Tg}* mice by cross *Csflr-Cre/Esr1^{Tg};Rs26^{fstdTomatt/tdTomato}* with *Colla1-GFP^{Tg}* mice. In this stain, collagen-producing cells would express green fluorescence protein (GFP) and *Csflr* expression cells would have tdtomato fluorescence after tamoxifen induction.

2.1.1.11 *Csflr-Cre/Esr1^{Tg};Rs26^{fstdTomato/+};Rs26^{iDTR/+}* mice

we generated *Csflr-Cre/Esr1^{Tg};Rs26^{fstdTomato/+};Rs26^{iDTR/+}* mice by cross *Csflr-Cre/Esr1^{Tg};Rs26^{fstdTomatt/tdTomato}* with *Rs26^{iDTR/iDTR}* mice. In this stain, *Csflr* expression cells would have tdtomato fluorescence and human DT receptor after tamoxifen induction.

All studies were carried out under a protocol approved by Institutional Animal Care and Use Committee, National Taiwan University College of Medicine



2.1.2 Diphtheria toxin (DT)

Mice were administrated Diphtheria toxin (0.5mg/vial; Sigma-Aldrich Co. LLC., St. Louis, Mo, USA) via intraperitoneal injection with the dose of 0, 25, 50ng/g of body weight every other day for total 3 times.

2.1.3 Chemicals

Name	Information
100 bp DNA ladder	Cat. ADM100.500, Arrowtec Limited, Berkshire, RG46XJ, UK
Agarose	Cat. A9539, Sigma-Aldrich Co. LLC., St. Louis, MO, USA
Bovine serum albumin (BSA)	Cat. ALB001, BioShop Canada Inc., Burlington, Ontario, Canada
Chloroform: Isoamylalcohol 24:1	Cat. C0549, Sigma-Aldrich Co. LLC., St. Louis, MO, USA
4',6'-Diamidino-2-phenylindole dihydrochloride (DAPI)	Cat. D1306, Molecular Probes, Life Technologies, Thermo Fisher Scientific Inc., USA
Diethyl pyrocarbonate (DEPC)	Cat. D-5758, Sigma-Aldrich Co. LLC., St. Louis, MO, USA
Dullbecco's modified eagle medium (DMEM)	Cat. 12100-046, Gibco, Life Technologies, Thermo Fisher Scientific Inc., USA
Dullbecco's modified eagle medium, a nutrient mixture F-12 powder (DMEM/F12)	Cat. 12400-024, Gibco, Life Technologies, Thermo Fisher Scientific Inc., USA

Ethelenediaminetetraacetic acid (EDTA)	Cat. E-5134, Sigma-Aldrich Co. LLC., St. Louis, MO, USA
Ethanol absolute	Cat. 32221, Sigma-Aldrich Co. LLC., St. Louis, MO, USA
DNeasy [®] Blood & Tissue kit (50)	Cat. 69504, Qiagen GmbH, Hilden, Germany
Fetal bovine serum (FBS)	Cat. 26140-079, Gibco, Life Technology, Green Island, NY, USA
Formalin solution, neutral buttered, 10%	Cat. HT501128, Sigma-Aldrich Co. LLC., St. Louis, MO, USA
Heparin LEO 5000 i.u./ml	LEO, Pharma A/S, Ballerup, Denmark
iQ [™] SYBR [®] green supermix	Cat. 170-8882AP, Bio-Rad Laboratories Inc., Hercules, CA, USA
iScript [™] cDNA synthesis kit	Cat. 170-8891, Bio-Rad Laboratories Inc., Hercules, CA, USA
Isoflurane	Panion & BF Biotech Inc., Taoyuan, Taiwan
Isopropanol	Cat. A10335-0500, Bionovas Biotechnology Co. Ltd., Toronto, Ontario, Canada
Ketalar [®] injection 50 mg/mL	Pfizer Inc., New York, NY, USA
L-Lysine monohydrochloride (Lysine: HCl)	Cat. L-5626, Sigma-Aldrich Co. LLC., St. Louis, MO, USA
Lysing Buffer	Cat. 555899, BD Biosciences, San Jose, CA, USA
Normal goat serum (NGS)	Cat. 005-000-121, Jackson ImmunoResearch Laboratories Inc., West Grove, PA, USA
Normal mouse serum	Cat. 015-000-120, Jackson ImmunoResearch Laboratories Inc., West Grove, PA, USA
Paraformaldehyde (PFA)	Cat. 441244, Sigma-Aldrich Co. LLC., St. Louis, MO, USA
Phosphate buffer solution (PBS) pH7.4 (10X)	Cat. 70011-044, Gibco, Life Technologies, Thermo Fisher Scientific Inc., USA
Potassium chloride (KCl), crystal	Cat. 3040-01, J.T. Baker [®] , Avantor

	Performance Materials Inc., Phillipsburg, NJ, USA
Potassium phosphate (KH ₂ PO ₄)	Cat. CK-CP1580153, One-Star Biotechnology Co. Ltd., Taipei, Taiwan
ProLong [®] Gold antifade reagent	Cat. P36934, Molecular Probes, Life Technologies, Thermo Fisher Scientific Inc., USA
Proteinase K	Cat. V3021, Promega Corporation, Madison, WI, USA
RNeasy [®] mini kit	Cat. 74106, Qiagen GmbH, Hilden, Germany
Sodium dodecyl sulfate (SDS)	Cat. 75746, Sigma-Aldrich Co. LLC., St. Louis, MO, USA
Sodium azide (NaN ₃)	Cat. S-8032, Sigma-Aldrich Co. LLC., St. Louis, MO, USA
Sodium chloride (NaCl), crystal	Cat. 3624-05, J.T. Baker [®] , Avantor Performance Materials Inc., Center Valley, PA
Sodium (meta) periodate	Cat. S1878, Sigma-Aldrich Co. LLC., St. Louis, MO, USA
Sodium phosphate dibasic (Na ₂ HPO ₄)	Cat. S3264, Sigma-Aldrich Co. LLC., St. Louis, MO, USA
Sodium phosphate monobasic (NaH ₂ PO ₄)	Cat. S3139, Sigma-Aldrich Co. LLC., St. Louis, MO, USA
Sucrose	Cat. AS1560-1000, Bionovas Biotechnology Co. Ltd., Toronto, Ontario, Canada
SyBR [®] safe DNA gel stain	Cat. S33102, Invitrogen [™] , Life Technologies, Thermo Fisher Scientific Inc., USA
Taq DNA polymerase 2x master mix RED	Cat. A180306, Ampliqon A/S, Odense M, Denmark
Tissue-Tek [®] O.C.T Compound	Cat. 4583, Sakura Finetek USA., Inc., Torrance, CA, USA
Tris (base)	Cat. 4109-02, J. T. Baker, Avantor

	Performance Materials, Inc., Center Valley, PA, USA
Tris hydrochloride (Tris-HCl)	Cat. 4103-02, J. T. Baker, Avantor Performance Materials, Inc., Center Valley, PA, USA
TRIzol [®] reagent	Cat. 15596018, Ambion, Life Technologies, Thermo Fisher Scientific Inc., USA
VECTASHIELD [®]	Cat. H-1000, Vector Laboratories, Inc., Burlingame, CA, USA
Xylazine hydrochloride	Cat. X1251, Sigma-Aldrich Co. LLC., St. Louis, MO, USA

2.1.4 Buffers

FACS buffer


Chemicals and reagent	Quantity	Final concentration
10x PBS	100 mL	1x
FBS	50 mL	5 %
10 % NaN ₃	10 mL	0.1 %
ddH ₂ O	Add to 1 L	

FACS wash buffer

Chemicals and reagent	Quantity	Final concentration
10x PBS	100 mL	1x
BSA	1 g	0.1 %
10 % NaN ₃	10 mL	0.1 %
ddH ₂ O	Add to 1 L	

Periodate-lysine-paraformaldehyde (PLP) solution 200mL

Chemicals and reagent	Quantity	Final concentration
-----------------------	----------	---------------------



0.1 M PB	75 mL	37.5 mM
ddH ₂ O	75 mL	
8 % PFA	50 mL	2 %
L-Lysine monohydrochloride	2.192 g	60 mM
Sodium (meta) periodate	0.428 g	10 mM
Sucrose	10 g	145.8 mM

Phosphate buffer (PB) 0.1M 200mL

Chemicals and reagent	Quantity	Final concentration
0.2 M NaH ₂ PO ₄	19 mL	19 mM
0.2 M Na ₂ HPO ₄	81 mL	81 mM
ddH ₂ O	Add to 200 mL	

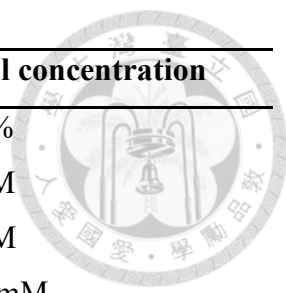
Phosphate buffered saline (PBS) (10x) 1L

Chemicals and reagent	Quantity	Final concentration
NaCl	80 g	1.37 M
Na ₂ HPO ₄	14.2 g	0.1 M
KCl	2 g	26.8 mM
KH ₂ PO ₄	2.4 g	17.6 mM
HCl	Adjust to pH 7.4	
ddH ₂ O	Add to 1 L	

Sorting Buffer 50mL

Chemicals and reagent	Quantity	Final concentration
0.5 M EDTA	200 μL	2 mM
FBS	0.5 mL	1 %
1x PBS pH 7.4	Add to 50 mL	

Tail Lysis Buffer 200mL



Chemicals and reagent	Quantity	Final concentration
10 % SDS	4 mL	0.2 %
1 M Tris pH 8.5	20 mL	0.1 M
0.5 M EDTA pH 8.0	2 mL	5 mM
NaCl	2.36 g	200 mM

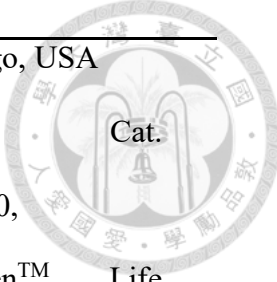
TE Buffer 50mL

Chemicals and reagent	Quantity	Final concentration
0.5 M EDTA pH 8	0.1 mL	1 mM
1 M Tris-HCl pH 7.5	0.5 mL	10 mM
ddH ₂ O	Add to 50 mL	

2.1.5 Antibodies

Primary antibodies

Name	Host	Information
Anti-CD11b 0.5 mg/mL	Rat	1:200, Cat. 14-0112, eBioscience, Inc., San Diego, USA
Anti-wide spectrum cytokeratin antibody	Rabbit	1:200, Cat. Ab9377, Sigma-Aldrich
Anti-Laminin antibody 0.5 mg/mL	Rabbit	1:400, Cat. L9393, Sigma-Aldrich Co. LLC., St. Louis, MO, USA
Anti-mouse CD45 PerCP- Cy5.5	Rat	1:200, Cat. 45-0451 eBioscience, Inc.,



0.2mg/mL			San Diego, USA
Anti-mouse F4/80	Rat	1:200,	Cat.
0.2 mg/mL		MF48000,	Invitrogen™, Life
			Technologies,
		Thermo	Fisher
		Scientific Inc.,	USA
Anti-Nidogen	Rat	1:200,	Cat. Sc-
0.2mg/mL		33706Santa	Cruz
		Biotechnology,	
		SantaCruz,CA	
Anti-Vimentin	Rat	1:200,	Cat sc7557,
0.2mg/mL		Santa	Cruz
		Biotechnology,	
		SantaCruz,CA	

Secondary antibodies

Name	Information
Alexa Fluor® 488 conjugated AffiniPure Goat Anti-Rat IgG (H+L)	1:400, Cat. 112-545-167, ImmunoResearch Laboratories Inc., West Grove, PA, USA
Alexa Fluor® 488 conjugated AffiniPure Goat Anti-Rabbit IgG (H+L)	1:400, Cat. 111-545-144, ImmunoResearch Laboratories Inc., West Grove, PA, USA

Alexa Fluor [®] 647	1:400, Cat. 111-606-144,
conjugated AffiniPure Goat	ImmunoResearch Laboratories Inc.,
Anti-Rabbit IgG (H+L)	West Grove, PA, USA
Cy TH 3-conjugated	1:400, Cat. 112-165-167,
AffiniPure Goat Anti-Rat	ImmunoResearch Laboratories Inc.,
IgG (H+L)	West Grove, PA, USA
Cy TH 3-conjugated	1:400, Cat. 111-165-144,
AffiniPure Goat Anti-	ImmunoResearch Laboratories Inc.,
Rabbit IgG (H+L)	West Grove, PA, USA

Fluorescence-conjugated primary antibodies

Name	Information
Anti-mouse CD45 PerCP-Cy5.5	1:200, Cat. 45-0451
0.2mg/mL	eBioscience, Inc., San Diego, USA
Anti-mouse CD11b FITC	1:400, Cat. 101205
0.5mg/mL	BioLegend, Inc., San Diego, CA, USA
Anti-mouse CD115 APC	1:200, Cat. 135509
0.2mg/mL	BioLegend, Inc., San Diego, CA, USA
BV421 Rat Anti-mouse	1:200, Cat. 565411
F4/80	BD Biosciences, San Jose, CA, USA
0.2mg/mL	



BV605 Rat Anti-mouse I-A/I-E (MHC classII)	1:200, Cat. 563413
0.2mg/mL	BD Biosciences, San Jose, CA, USA
α SMA-Cy3	1:200, C6198
mouse	Sigma-Aldrich Co. LLC., St. Louis, MO, USA
α SMA-FITC	1:200, F3777
mouse	Sigma-Aldrich Co. LLC., St. Louis, MO, USA

2.1.6 Instruments

Name	Information
BD FACS Aria TM IIIu	BD Biosciences, San Jose, CA, USA
BD FACSCalibur TM	BD Biosciences, San Jose, CA, USA
BD LSRFortessa TM	BD Biosciences, San Jose, CA, USA
CFX Connect TM Real-Time PCR Detection System	Cat. 185-5201, Bio-Rad Laboratories, Inc., Hercules, CA, USA
Cryostat	Leica CM 1950, Leica Microsystems GmbH, Wetzlar, Germany
Homeothermic Blanket System	Cat. 50300, Stoelting Co., IL, USA.
Leica TCS SP5	Cat. DM5000B, Leica Microsystems GmbH, Wetzlar, Germany
My iQ TM Single Color Real-Time PCR Detection System	Cat. 170-9740, Bio-Rad Laboratories, Inc., Hercules, CA, USA
MultiGene Thermal Cycler	Cat. TC9600-G, Labnet International, Inc., Edison, NJ, USA
NanoDrop 2000 Spectrophotometer	UV-Vis Cat. ND-2000, Thermo Fisher Scientific Inc., Waltham, MA, USA

T100™ Thermal Cycler	Cat. 186-1096, Bio-Rad Laboratories, Inc., Hercules, CA, USA
Carl Zeiss LSM880 (with Airyscan)	Cat. AxioImager. Z2, Zeiss, Oberkochen, Germany
Carl Zeiss LSM780	Cat. AxioObserver Z1, Zeiss, Oberkochen, Germany



2.2 Methods

2.2.1 Peritoneal fibrosis model

Adult mice (aged 14 weeks) were induced by an intraperitoneal injection of 50 ml/kg body weight of normal saline with 0.05% sodium hypochlorite.[10] After sodium hypochlorite administration, mice would be sacrificed at Day2, 4, and 7 for analysis.

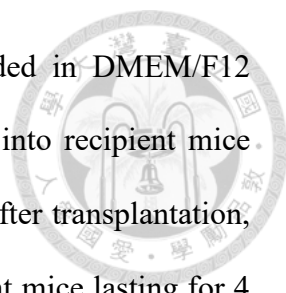
2.2.2 Chimeric mice model

2.2.2.1 Parabiosis

Parabiosis is a way to create a chimeric mice model which small mirror-image incisions are made along adjacent flanks of age-matched mice from elbow to thigh by using clips.

2.2.2.2 Bone marrow transplantation

Both femur and tibia bone of donor mice (male) were collected after sacrificed and the bone marrow cells were wash out with DMEM/F12



medium. The bone marrow cells were resuspended in DMEM/F12 medium after centrifuging and were transplanted into recipient mice which received 1000rad irradiation via tail vein. After transplantation, neomycin was added to drinking water for recipient mice lasting for 4 weeks.

2.2.3 Sample preparation

2.2.3.1 Tissue collection

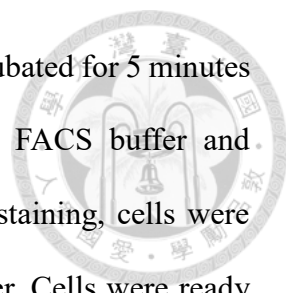
4% paraformaldehyde was administered into mice abdominal cavity after anesthesia. 3 minutes later, collect the abdominal muscle walls, great omentum, intestine and liver from mice. The tissue for immunofluorescence stain was soaked in PLP solution for 2 hours and then transfer to 18% sucrose solution for dehydration overnight. The tissue for immunohistochemistry stain was soaked in Formalin for preservation before paraffin embedding.

2.2.3.2 Isolation of peritoneal cells

Mice peritoneal cells were recovered by peritoneal cavity lavage with 8ml of ice-cold PBS after anesthesia.

2.2.4 Flow cytometry

Cells (Peritoneal lavage) were wash by ice-cold PBS and applied with Lysing buffer. Cells were washed by ice-cold PBS twice after RBC lysing and



resuspended in FACS buffer with FcR blocker and then incubated for 5 minutes at 4°C. Fluorescent-conjugated antibody was added into FACS buffer and incubated with cells for 30 minutes at 4°C in dark. After staining, cells were wash twice by wash buffer and resuspended in FACS buffer. Cells were ready for Flow cytometry after filtered with 40µm mesh.

2.2.5 Fluorescence-activated cell sorting (FACS) system

The specimen was prepared in Sorting buffer containing 5% FBS and EDTA in PBS. FACS Aria cell sorter (BD Biosciences, San Jose, CA) was applied to isolate specific population in specimen.

2.2.6 Immunofluorescence stain

Tissue was embedded with OCT and section into 5mm thickness. The slides were rinsed in 1x PBS for 5 minutes at room temperature and repeat twice. Blocking was done with 10% normal goat serum (NGS) in PBS for 30 minutes at room temperature. The slide was covered with blocking buffer (10% normal goat serum in PBS) containing diluted primary antibodies and incubated for 2 hours at room temperature. After washed in PBS for 3 times, fluorescence-conjugated affinity-purified secondary antibodies were prepared in 10% NGS and added to the sections for 30 minutes at room temperature. Diluted 4', 6-diamidino-2-phenylindole (DAPI) was used for nuclear staining for 2 minutes at room temperature. Following the final step of washing with PBS for 3 times, the slides were mounted with VECTASHIELD® (Vector Laboratories, USA), or ProLong® Gold antifade reagent (Molecular Probes, Life Technologies, Thermo

Fisher Scientific Inc., USA) for non-direct- conjugated or direct-conjugated antibodies respectively, and cover slips were sealed[104].



2.2.7 Masson's Trichrome stain

Masson's trichrome stain was performed in 4-mm-thick paraffin sections and the peritoneal membrane thickness on the liver surface was measured in 10 sections from every 10th section for each mouse (five randomly selected images per section).

2.2.8 Isolation of bone marrow cells and measurement of engraftment efficiency

As described above. Both femur and tibia bone of donor mice (male) were collected after sacrificed and the bone marrow cells were wash out with ice-cold PBS. QIAGEN DNeasy® Blood and Tissue Kit was used to get genomic DNA from recipient mice. Engraftment efficiency was confirmed by duplex qPCR using specific detection probes for Y-chromosome Y6 and autosomal GAPDH primer amplicons in bone marrow of recipient[105].

2.2.9 Statistical analysis

Statistical analyses of all experiments were carried out with GraphPad Prism 5 (GraphPad Software, Inc., La Jolla, CA, USA). One-way analysis of variance (ANOVA) is used to evaluate the statistical significance among three groups or more. A p value less than 0.05 is considered statistical significant.

Chapter 3 Results

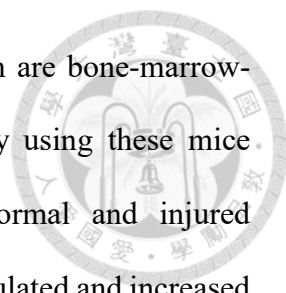


3.1 Identified subsets of macrophages in peritoneal cavity

To clarify the accumulated macrophages are from circulation or tissue-resident, we first analyzed the subsets of macrophages in peritoneal cavity. We followed the previous studies[89, 91] to divide peritoneal macrophage into two distinct group, large peritoneal macrophages (LPM, $CD11b^{hi}F4/80^{hi}MHCII^{low}$) and small peritoneal macrophages (SPM, $CD11b^{hi}F4/80^{low}MHCII^{hi}$) based on the expression of CD11b, F4/80, and major histocompatibility complex class II (MHCII). LPM were the most abundant macrophage subset (93.2 %) in unstimulated mice; SPM accounted for the remaining part of the peritoneal macrophages. Activation of *Csf1r*-Cre recombinase shown by expression of tdTomato red fluorescence protein (RFP) was induced in 65% of $CD11b^{hi}$ peritoneal macrophages of *Csf1r-Cre/Esr1^{Tg};Rs26^{stdTomato/+}* mice. Previous study indicated that monocyte-derived macrophages could be a source of SPM during peritoneal injury[89], which means SPM are from circulation. In contrast, LPM are more like tissue-resident macrophages, which can slowly self-renew in steady state[79, 80].

3.2 Macrophage increased in injured peritoneum

Csf1r-Cre/Esr1^{Tg};Rs26^{stdTomato/+} mice expressed RFP in *Csf1r*-expressing cells, such as peritoneal macrophages shown in Figure 1A, after tamoxifen administration. In addition, Cre-mediated recombination of the LoxP flanked



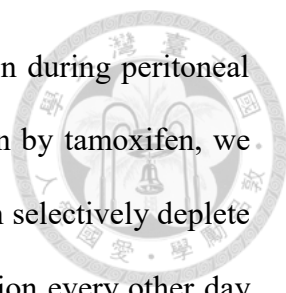
sequences is also activated in *Csf1r*-expressing cells which are bone-marrow-derived macrophages and yolk sac macrophages[106]. By using these mice models, we could study peritoneal macrophages in normal and injured peritoneum (Figure 2A). We found that macrophages accumulated and increased in injured peritoneum at D4 and D7 after sodium hypochlorite injection compared to normal condition (Figure 2B and C).

3.3 Macrophage ablation by diphtheria toxin

To understand the role of peritoneal macrophages in peritoneal fibrosis, we generated mice (*Csf1r-Cre/Esr1^{Tg};Rs26^{iDTR/+}*) with macrophage-specific expression of diphtheria toxin receptor (DTR) by breeding *Csf1r-Cre/Esr1^{Tg}* mice with *Rs26^{iDTR/iDTR}* mice. Based on the recombination efficiency shown in *Csf1r-Cre/Esr1^{Tg};Rs26^{stdTomato/+}* mice after tamoxifen administration (Figure 1A), we expected DTR would express in 65% of *Csf1r*-expressing macrophages in *Csf1r-Cre/Esr1^{Tg};Rs26^{iDTR/+}* mice. Two weeks after tamoxifen administration, DT of 25 ng/g body weight was administrated into mice every other day via retro-orbital injection from day 2 to 6 after peritoneal hypochlorite injury (Figure 3A). By flow cytometric analyses, not only the cell counts of CD11b^{hi} macrophages but also the percentage of CD11b^{hi} macrophages in harvested peritoneal cells decreased by DT injection at day 7 after peritoneal hypochlorite injury although no significant change was found at day 3 and 5 (Figure 3B, C).

3.4 Macrophage ablation attenuated peritoneal fibrosis

We generated *Csf1r-Cre/Esr1^{Tg};Rs26^{stdTomato/+};Rs26^{iDTR/+}* mice to visualize

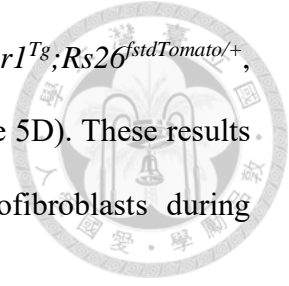


Csf1r-RFP⁺ macrophages and deplete them by DT injection during peritoneal injury. Two weeks after activation of genetic recombination by tamoxifen, we induced peritoneal fibrosis by sodium hypochlorite and then selectively deplete Csf1r-expressing macrophages by intraperitoneal DT injection every other day from day 2 after peritoneal injury (Figure 4A). Analyses of Csf1r-RFP⁺ macrophages and α SMA⁺ myofibroblasts by immunofluorescence showed that cell numbers of myofibroblasts were reduced with the ablation of macrophages (Figure 4B and 4C). The severity of peritoneal fibrosis assessed by the thickness of peritoneum on the surfaces of livers and abdominal muscle walls in Masson's trichrome stain was reduced DT dose-dependently (Figure 4D-F). These experiments indicated that macrophages play a role in the accumulation of α SMA⁺ myofibroblasts and extracellular matrix during peritoneal fibrosis either by differentiation into collagen-producing cells or by cross talk with SM fibroblasts to promote their transition into myofibroblasts.

3.5 Macrophages did not produce collagen and α -SMA in injured peritoneum

To understand whether peritoneal macrophages produced collagen before and after hypochlorite injury, we generated *Csf1r-Cre/Esr1^{Tg};Rs26^{fstdTomato/+};Coll1a1-GFP^{Tg}* mice whose collagen-producing cells would express green fluorescence protein (GFP) (Figure 5A). Our data showed that Csf1r-RFP⁺ macrophages expressed Coll1a1-GFP in neither normal nor fibrotic peritoneum (Figure 5B, C), suggesting that macrophages did not produce collagen and cause scar formation directly even in injured peritoneum. We

further analyzed $Csf1r$ -RFP⁺ macrophages by using $Cre/Esr1^{Tg};Rs26^{stdTomato/+}$, and we found that $Csf1r$ -RFP⁺ macrophages neither (Figure 5D). These results indicating that macrophages did not transition into myofibroblasts during peritoneal fibrosis.



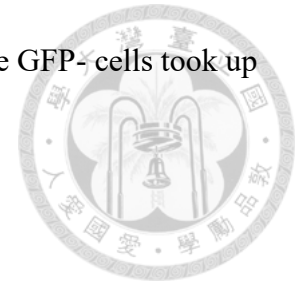
3.6 Chimeric mice were generated by parabiosis

To study the role of circulating monocyte-derived macrophages in peritoneal fibrosis, we used parabiosis to generate chimeric mice. To confirm the development of cross-circulation between two mice, we used $CAG-EGFP^{Tg}$ mice and wild type (WT) $C57BL/6$ mice to perform parabiosis surgery (Figure 6A) and analysis of the peripheral blood by flow cytometry at day 16 after surgery. We found that 50.39% of the CD45⁺ cells in peripheral blood of WT mice were GFP⁺, suggesting the development of cross-circulation in the parabiont (Figure 6B).

3.7 Circulating monocytes-derived macrophages recruited to peritoneal cavity after injury

To figure out whether monocyte-derived macrophages recruit to peritoneal cavity, we used $Rs26-EGFP^{Tg}$ mice and wild type (WT) $C57BL/6$ mice to perform parabiosis surgery and analysis of the peritoneal cavity cells by flow cytometry four weeks after surgery (Figure 7A). After hypochlorite injury, we used CD11b as macrophage marker and found that 20.4% were GFP⁻ cells and 79.5% were GFP⁺ cells in CD11b positive population in $Rs26-EGFP^{Tg}$ mice (Figure 7B). This result suggested that 40% of circulating monocyte-derived

macrophages recruit to peritoneal cavity after injury because GFP- cells took up 50% in peripheral blood in parabiont (Figure 7C, D).



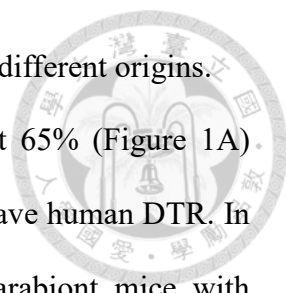
3.8 Macrophage ablation in parabiosis model

To study the role of circulating monocyte-derived macrophage, we use *Csf1r-Cre/Esr1^{Tg};Rs26^{iDTR/+}* (label as Cre/iDTR) and littermate control (without Cre and human DTR, label as +/iDTR) to generate chimeric mice (Figure 6C). Based on the flow cytometric analysis in parabiont *CAG-EGFP^{Tg}-WT C57BL/6* (Figure 6B), the microcirculation between two mice were established 2-3 weeks after parabiosis surgery, indicating the same blood was shared in the peripheral circulation. Thus, monocytes with human DTR would exist in both parabiont mice. However, the peritoneal macrophages would not be affected after parabiosis, indicating the parabionts preserved their own macrophages[107]. DT were intraperitoneally administrated at day 2, 4, 6 after hypochlorite injury (Figure 8A). We expected that peritoneal fibrosis in both of parabiont mice with DT administration would be attenuated since that monocytes with human DTR exist in their peripheral blood. However, we didn't find that any difference between parabiont mice with vehicle or DT administration in cell numbers of CD11b⁺ macrophages and α SMA⁺ myofibroblasts (Figure 8B, C) Masson's trichrome staining also showed no difference in the thickness of peritoneal membranes covering the surface of livers and muscle walls in injured peritoneum of both parabiont mice with control or DT injection (Figure 8D, E).

Chapter 4 Discussion

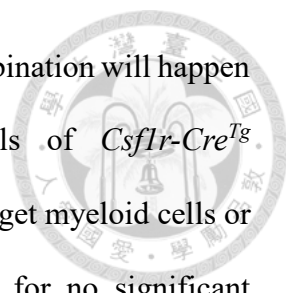


In 2016, Wang S et al. used cell lineage tracing to adoptive transfer of GFP⁺ or dye-labelled macrophages, and found that identified that monocyte/macrophages from bone marrow can give rise to myofibroblasts via the process of macrophage-myofibroblast transition (MMT) in a mouse model of unilateral ureteric obstruction[108]. They claimed that MMT cells were a major source of collagen-producing fibroblasts in the fibrosing kidney, accounting for more than 60% of α -SMA⁺ myofibroblasts[108, 109]. However, we didn't find any Csf1r-RFP⁺ cells express α -SMA or collagen (Figure 5B-D) in peritoneal fibrosis model. Besides, our previous study proved that peritoneal myofibroblasts derive from submesothelial (SM) fibroblasts[109] instead of mesothelial cells. As a consequence, the reasons that peritoneal fibrosis was attenuated after macrophage ablation might be the breakdown of profibrotic signaling from macrophages to myofibroblasts. Previous study showed that macrophages undergo phenotype-switch after peritoneal injury and secrete many inflammatory cytokines including CXCL1, CXCL2, CCL2, TNF- α , IL-6, etc[93]. Among these cytokines, TNF- α was thought to increase myofibroblasts proliferation during injury[110, 111]. Previous study also showed that TNF- α can activate the proliferation and prolong the survival of myofibroblast[96]. This could be one of the reasons that peritoneal fibrosis was attenuated after macrophage ablation in our study. Regarding the significance of LPM and SPM in peritoneal fibrosis and the contribution of circulation-derived macrophages to LPM/SPM, more study will be needed. Moreover, we also need more study to explore the profibrotic signaling from macrophages to myofibroblasts during



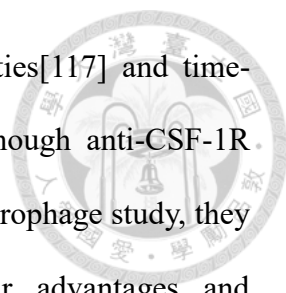
peritoneal injury and the role of specific macrophages from different origins. The recombination efficiency of *Csf1r-cre/Esr1* was about 65% (Figure 1A) which means that only 65% of macrophages (monocytes) have human DTR. In parabiosis study, we observed similar results between parabiont mice with vehicle or DT administration in cell numbers of CD11b⁺ macrophages and α SMA⁺ myofibroblasts (Figure 7B-D). We suggested that the low recombination efficiency of *Csf1r-cre/Esr1* was the major reason causing no differences between control and DT group. In parabiosis study, the parabionts would share peripheral circulation, then 32.5% of monocytes would express human DTR in both parabionts *+/iDTR* and *Cre/iDTR* (Figure 6C). Because only 40% of peritoneal macrophages derived from circulation, the peritoneal macrophages expressing human DTR in the *+/iDTR* mice would be about 13% which might lead to insignificant ablation of macrophages and no effect on peritoneal fibrosis. However, more than 50% of peritoneal macrophages in parabiont *Cre/iDTR* mice might express human DTR and be susceptible to ablation by DT, including 39% from expanded resident macrophages (62.5% recombination x 60% from resident macrophages) and 13% from circulation, the lack of significant effect of macrophage ablation in *Cre/iDTR* parabiont might suggest the ignorable role of resident macrophages in peritoneal fibrosis. However, the conclusion needs more delicate experiments to prove.

To overcome the issue of recombination efficiency of *Csf1r-cre/Esr1* induced by tamoxifen, we can use *LysM^{Cre/+}* (JAX#004781) or *Csf1r-Cre^{Tg}* (JAX# 029206) mice to breed with *Rs26^{iDTR/iDTR}* mice. Cre-mediated recombination happens in the lysozyme2 gene in the myeloid cell lineage, including monocytes, mature



macrophages, and granulocytes. However near 100% recombination will happen in monocytes/macrophages, conventional dendritic cells of *Csf1r-Cre^{Tg}* mice[112]. These strains provide a more powerful tool to target myeloid cells or monocytes/macrophages. As discussed above, the reason for no significant ablation of CD11b^{hi} macrophages of *Csf1r-Cre/Esr1^{Tg};Rs26^{fsiDTR/+}* mice at day 3 and 5 after hypochlorite injury was not clear. *LysM^{Cre/+};Rs26^{iDTR/+}* or *Csf1r-Cre^{Tg};Rs26^{iDTR/+}* might provide a chance to check whether recombination efficiency is one of the reasons.

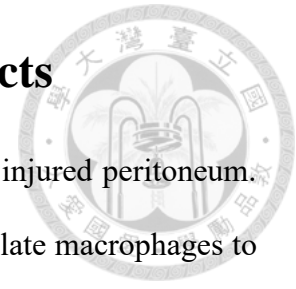
In contrast to our approaches, use of inhibitors directed against the protein tyrosine kinase activity of the CSF1R or agents that block the binding of CSF-1 are commonly applied in many other studies[113]. One of the studies demonstrated that CSF1R blockade reduced the resident macrophages and tumor-associated macrophages in syngeneic tumor models[114]. Conversely, it had no effect on inflammatory monocyte recruitment in models, including lipopolysaccharide-induced lung inflammation, wound healing, peritonitis, and severe acute graft-versus-host disease[114]. As a consequence, the investigators claimed that CSF-1R is not a good target for anti-inflammatory therapy since that high levels of CSF-1 seen in many inflammatory diseases are probably a part of a feedback damage repair response, and on that basis it could even be counterproductive to target the receptor[113-115]. However, in our study, we used *Csf1r-Cre/Esr1^{Tg};Rs26^{iDTR/+}* transgenic mice to ablate the CSF1R positive cell which might reduce effects of the feedback production of receptors. Anti-CSF-1 antibodies are less used compared to anti-CSF-1R antibodies in blocking CSF-1 signaling. Many studies found that postnatal neutralized CSF-1 signaling



causes growth retardation[116], developmental abnormalities[117] and time-dependent loss of Kupffer cells from the liver[118]. Although anti-CSF-1R blockade and anti-CSF1 mAb provide another tools for macrophage study, they still have many problems to overcome. Overall their advantages and disadvantages, transgenic mice with potential to ablate macrophages genetically might be better approaches.

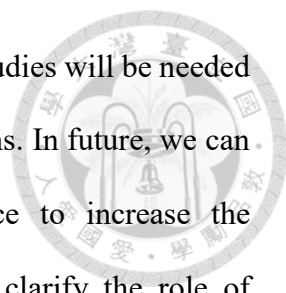
Compared to PDF and SES model, sodium hypochlorite induced peritoneal fibrosis was a rapid and effective method. However, the inconsistency in severity of peritoneal injury and difficulty in quantification exist in all of these models. Therefore, it was difficult to evaluate the effectiveness of treatments. Developing a stable model of peritoneal fibrosis is an important issue in the future. Using peritoneal function study including equilibration test, quantification cytokine concentration and image study (CT and MRI imaging) to evaluate the injury of peritoneum might be another approaches.

Chapter 5 Conclusion and future prospects



We first observed that many macrophages accumulated in injured peritoneum. Thus, we generated *Csf1r-Cre/Esr1^{Tg};Rs26^{iDTR/+}* mice to ablate macrophages to understand their roles during peritoneal fibrosis. We found that sodium hypochlorite-induced fibrosis could be attenuated after macrophage ablation. These results indicated that macrophages play an important character during peritoneal fibrosis. We further studied whether macrophages directly produce collagen within fibrosis process. However, we found that *Csf1r-RFP+* macrophages expressed *Colla1-GFP* (Figure 5B, C) and α -SMA (Figure 5D) in neither normal nor fibrotic peritoneum, indicating that MMT did not happen during peritoneal fibrosis. These results suggested that macrophage may cross talk to other peritoneal cells, especially submesothelial fibroblasts/myofibroblasts instead of directly producing collagen and scar. We further analyzed circulating and tissue-resident macrophages by using parabiosis model. We showed that about 40% of circulating monocyte-derived macrophages recruited to peritoneal cavity during peritoneal fibrosis (Figure 7). However, we didn't observe any difference between parabiont mice with vehicle or DT administration in cell numbers of CD11b⁺ macrophages and α SMA⁺ myofibroblasts in parabiosis surgery of *Csf1r-Cre/Esr1^{Tg};Rs26^{iDTR/+}* and littermate control possibly due to the low recombination efficiency of *Csf1r-cre/Esr1* (Figure 8B, C). Our data might also hint that resident macrophages play an ignorable role in peritoneal fibrosis. But the definite conclusion needs more studies to make.

In conclusion, our study implicated that macrophages have effects on peritoneal



fibrosis but not through a MMT pathway. However, more studies will be needed to define the clear role of macrophages from different origins. In future, we can use *LysM^{Cre/+}; Rs26^{iDTR/+}* or *Csf1r-Cre^{Tg};Rs26^{iDTR/+}* mice to increase the efficiency of genetic recombination and cell ablation to clarify the role of macrophages during peritoneal fibrosis. In addition, the profibrotic signals delivered by macrophages to fibroblasts for their proliferation and differentiation into myofibroblasts also need more studies. By using parabiosis of *CAG-EGFP^{Tg}* or *Rs26-EGFP^{Tg}* and wild type C57BL/6 mice, we can analyze the surface markers of GFP⁺ cell in wild type mice to study the circulating monocyte-derived macrophage phenotype switch and their functions during peritoneal fibrosis in further experiments.

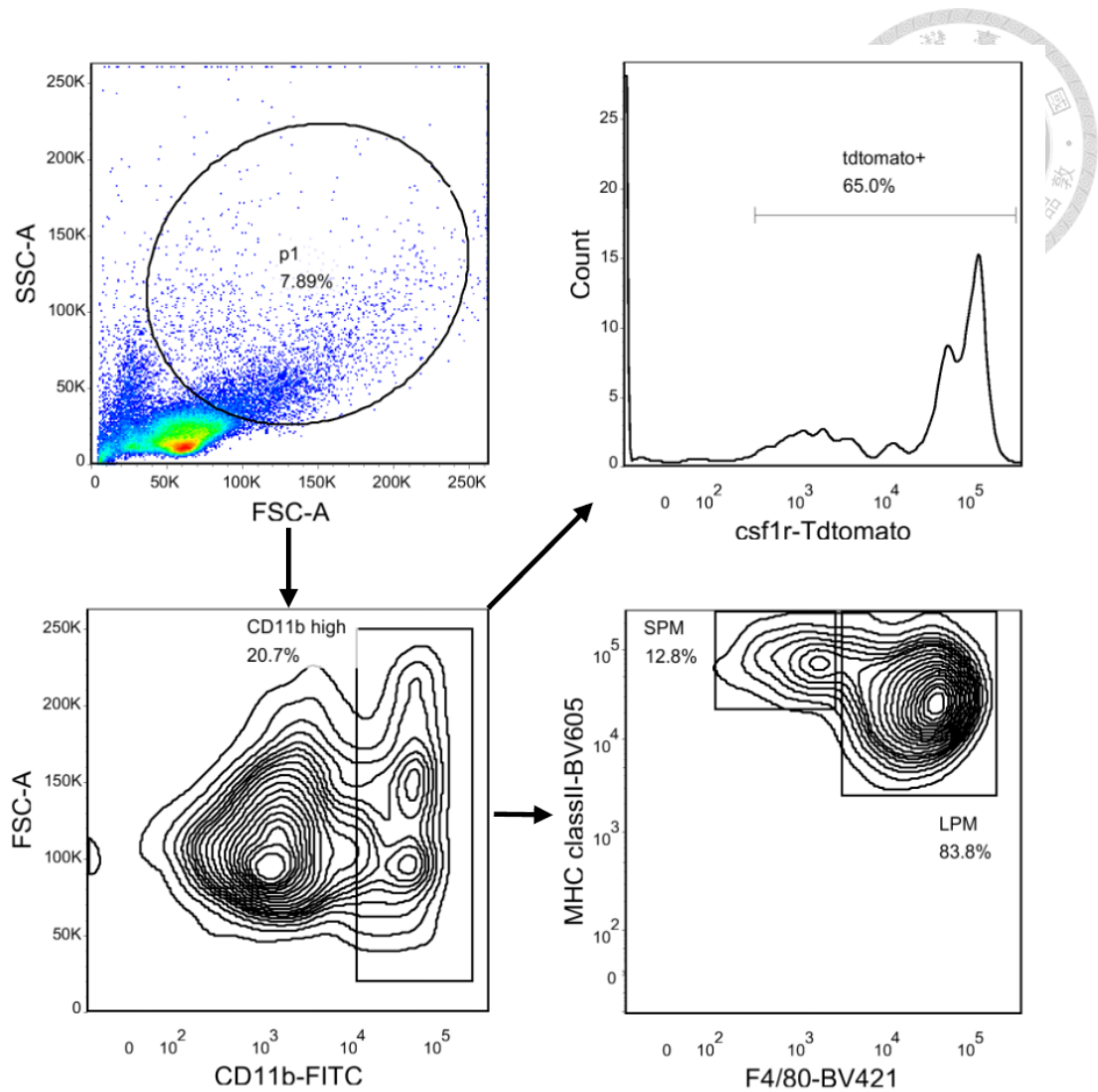
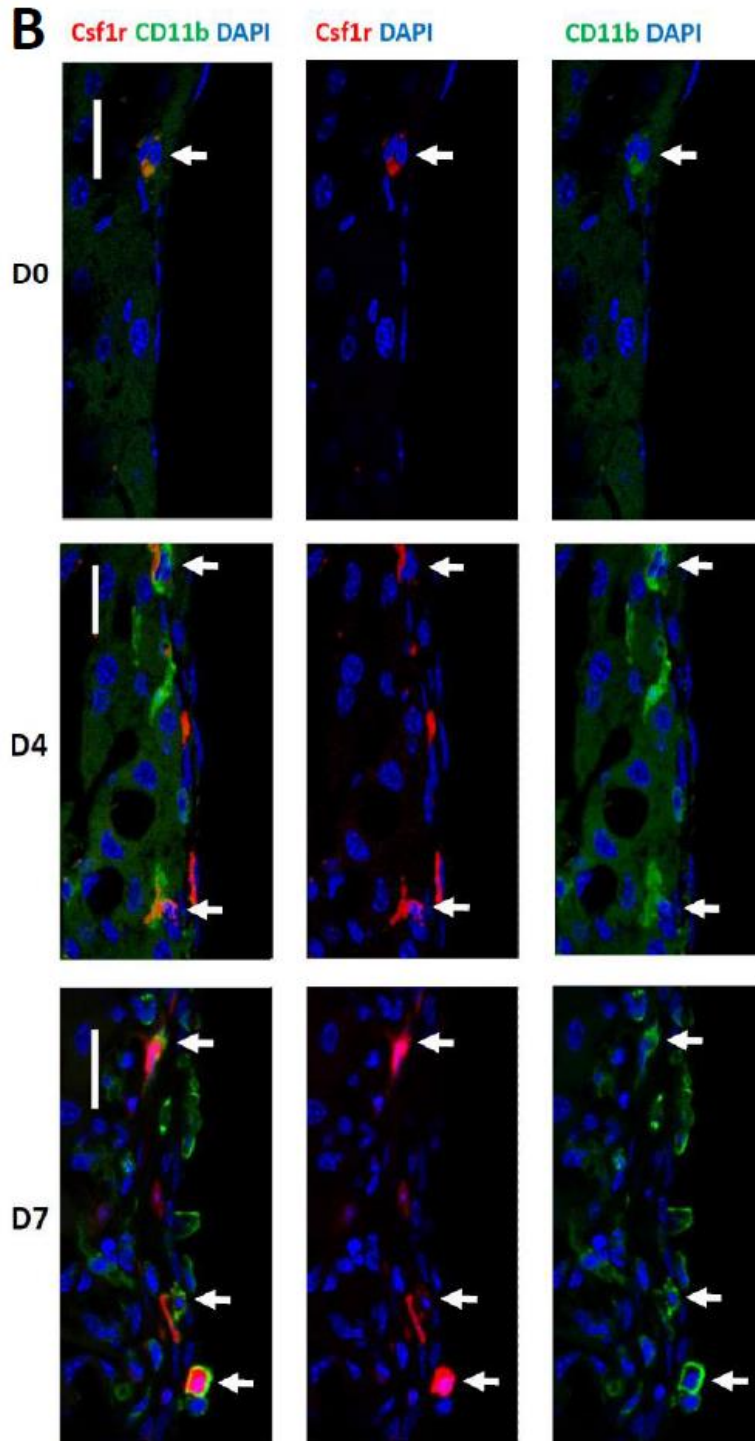
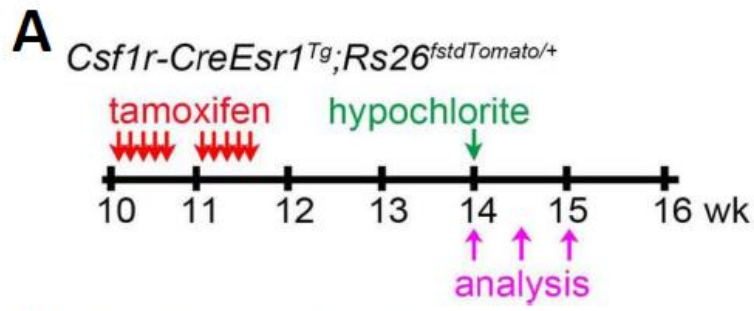


Figure 1

Flow cytometry analyses for macrophage subsets in peritoneal lavage cells of naïve *Csf1r-Cre/Esr1^{Tg};Rs26^{fltdTomato/+}* mice. In CD11b^{hi} population, large peritoneal macrophages (LPM) and small peritoneal macrophages (SPM) could be distinguished by using F4/80 and major histocompatibility complex (MHC) class II expression. LPM and SPM were CD11b^{hi}F4/80^{hi}MHCII^{low} and CD11b^{hi}F4/80^{low}MHCII^{hi}, respectively. In CD11b high population, 65% expressed *Csf1r*-RFP, indicating high activity of tamoxifen-induced *Csf1r*-Cre recombinase.



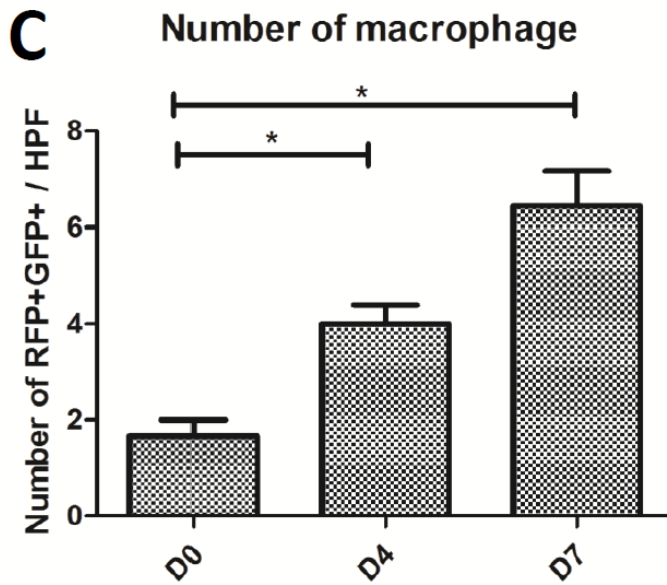


Figure 2

Macrophages increase in injured peritoneum.

(A) Experimental schema for tamoxifen administration, hypochlorite peritoneal injury and analyzed at day 4 and day7 after peritoneal injury. (B) By using *Csf1r-Cre/Esr1^{Tg};Rs26^{fstdTomato/+}* mice models, we found that many RFP+ and CD11b+ (arrow) macrophages accumulated and increased in injured peritoneum at D4 (middle) and D7 (lower) after sodium hypochlorite injection compared to normal condition upper). (C) Quantification of macrophages number at D0, D4 and D7

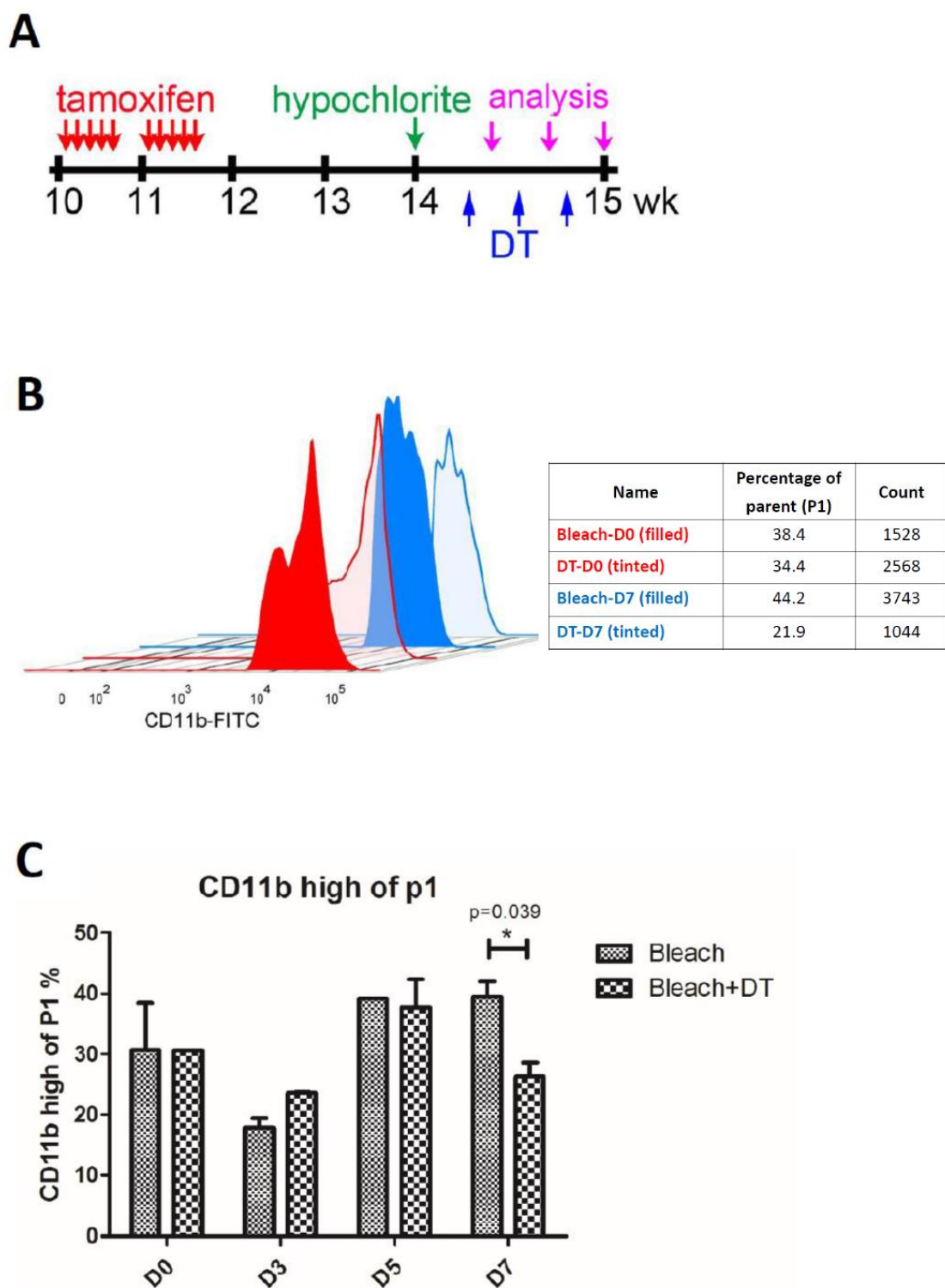
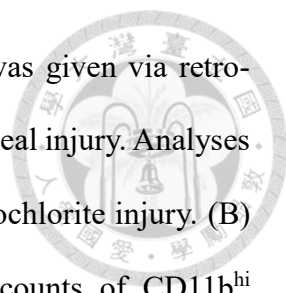


Figure 3

Macrophage ablation by diphtheria toxin. (A) Experimental schema for tamoxifen administration, hypochlorite peritoneal injury and diphtheria toxin



(DT) injection in *Csf1r-Cre/Esr1^{Tg}; Rs26^{iDTR/+}* mice. DT was given via retro-orbital injection every other day from day 2 to 6 after peritoneal injury. Analyses by flow cytometry were performed at day 3, 5, 7 after hypochlorite injury. (B) Representative flow cytometric analysis shows the cell counts of CD11b^{hi} macrophages before (D0) and at day 7 (D7) after hypochlorite injury with or without DT injection. The analyses were performed in P1 gated cells as shown in Figure 1. (C) Bar chart shows the percentage of CD11b^{hi} macrophages in harvested peritoneal cells before (D0) and Day 3, 5, 7 after hypochlorite injury and DT injections according to the experimental schema shown in (A). The percentage of CD11b^{hi} macrophages significantly decreased at Day 7 after DT administration. Data shown are representative of at least two experiments.

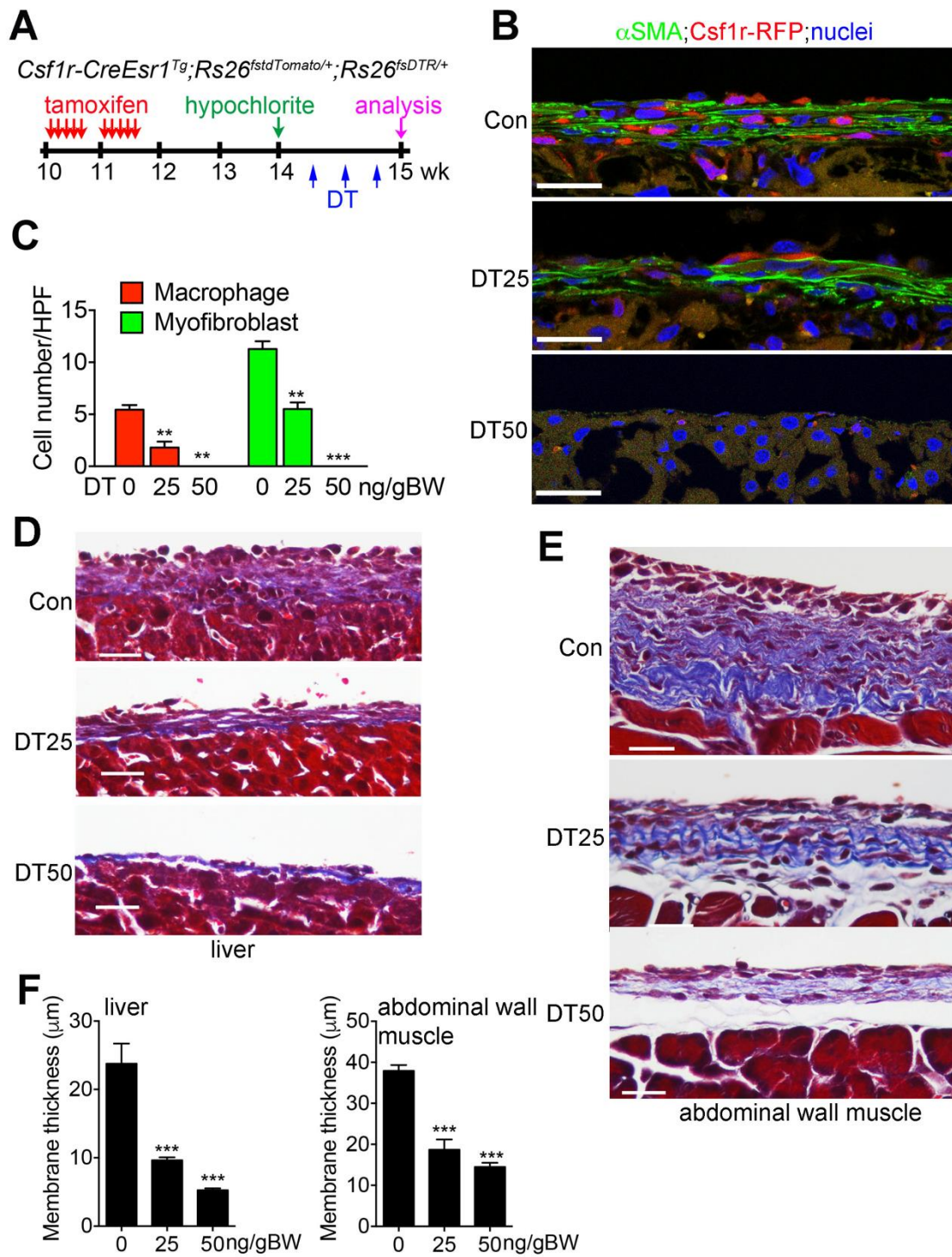


Figure 4

Macrophage ablation attenuated peritoneal fibrosis.

(A) Experimental schema for hypochlorite peritoneal injury and diphtheria toxin

injection in *Csf1r-Cre/Esr1^{Tg};Rs26^{fstdTomato/+};Rs26^{iDTR/+}* mice. Analyses were performed on the peritoneal covering of liver 7 days after hypochlorite injury followed by DT or PBS vehicle injection intraperitoneally every other day for 3 times from day 2 after peritoneal injury. (B) Images showed the cell number of α SMA⁺ myofibroblasts and *Csf1r*-RFP⁺ macrophages in the peritoneal coverings of livers at day 7 after peritoneal injury followed by intraperitoneal injections of PBS (Con), DT at doses of 25 (DT25) or 50 (DT50) ng/g body weight (BW) according to the experimental schema in (A). (C) Bar graph showed the cell numbers of macrophages and myofibroblasts in injured peritoneum with PBS control or DT injection (n=6 per group). (D and E) Images of Masson's trichrome stain showed thickness of peritoneal coverings of livers (D) and of muscle walls (E) after peritoneal injury followed by intraperitoneal injections of PBS (Con) and DT (DT25, DT50). (F) Bar graphs showed the thickness of peritoneal membrane covering the surface of livers and muscle walls in injured peritoneum with PBS control or DT injection (n=6 per group). Bar = 20 μ m. Original magnification, x630 and x400 in (B) and (D, E), respectively.

D day 7 after injury

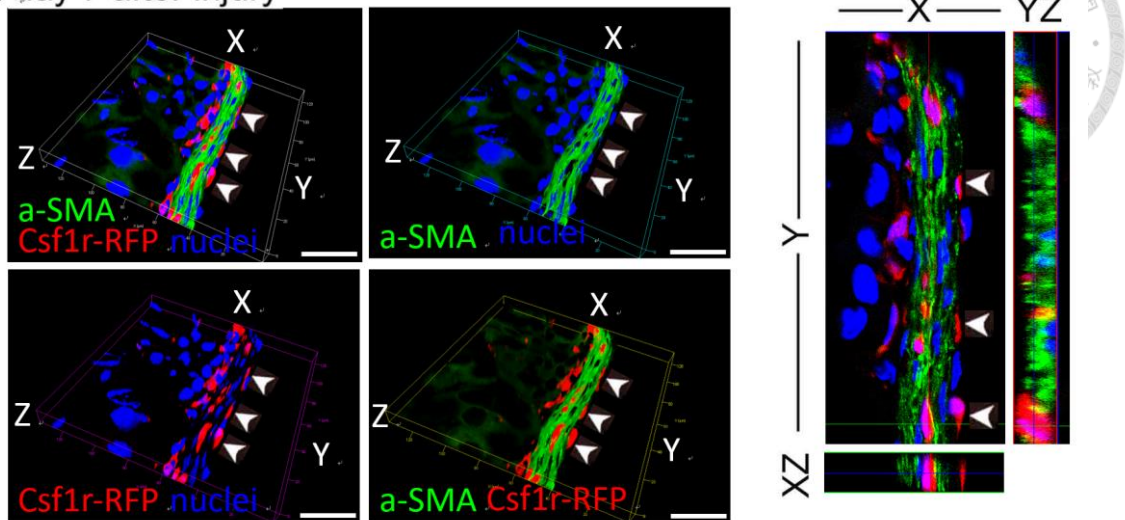


Figure 5

Macrophages did not produce collagen in injured peritoneum. (A) Experimental schema for cohort labeling of Csflr-RFP⁺ cells and hypochlorite peritoneal injury in *Csflr-Cre/Esr1^{Tg};Rs26^{stdTomato}/+;Colla1-GFP^{Tg}* mice. (B) Three dimension images with YZ and XZ stacks showed that tamoxifen-induced cohort labeling of Csflr-RFP⁺ macrophage (arrowhead) did not express Colla1-GFP (arrows) in normal peritoneum overlying liver. (C) Three-dimensional images with YZ and XZ stacks showed that Csflr-RFP⁺ macrophages (arrowhead) did not express Colla1-GFP (arrows) in thickened peritoneum overlying liver at day 7 after hypochlorite injury. (D) Three-dimensional images with YZ and XZ stacks showed that Csflr-RFP⁺ macrophages (arrowhead) did not express a-SMA in thickened peritoneum overlying liver at day 7 after hypochlorite injury. Bar = 20 μ m (in B, C), original magnification 630X.

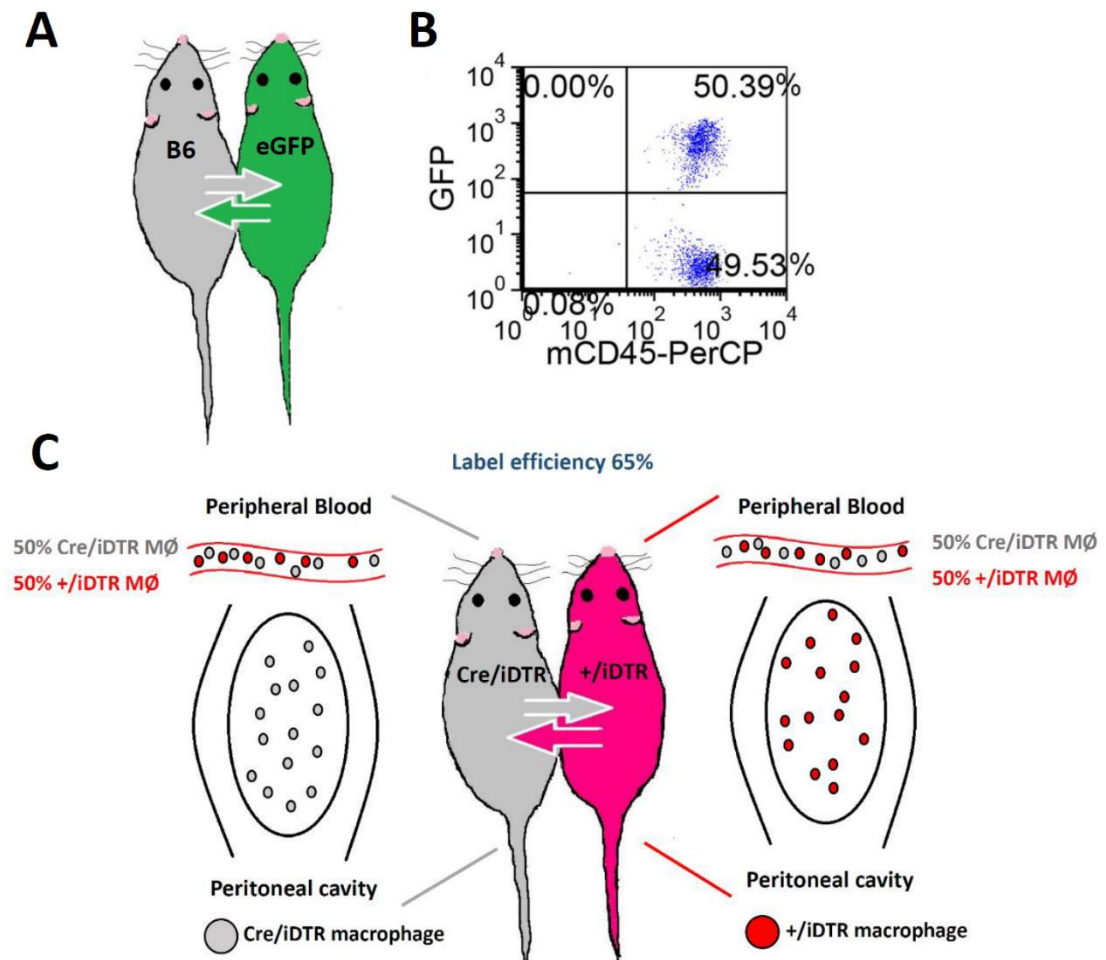


Figure 6

Chimeric mice were generated by parabiosis. (A) Parabiosis between *CAG-EGFP^{Tg}* and wild type C57BL/6 mice were generated by unilateral flank skin incision from elbow to the knee joints and then suture of skin edge by clips. (B) Representative flow cytometric analysis showed that 50.39% of CD45⁺ cells in peripheral blood of C57BL/6 mouse are GFP⁺ at day 16 after parabiosis surgery. (C) Schematic diagram of parabiosis between *Csf1r-Cre/Esr1^{Tg};Rs26^{iDTR/+}* (label as Cre/iDTR) and littermate control (without Cre and expression of human DTR, label as +iDTR) mice and distribution of macrophages in their peripheral blood and peritoneal cavity.

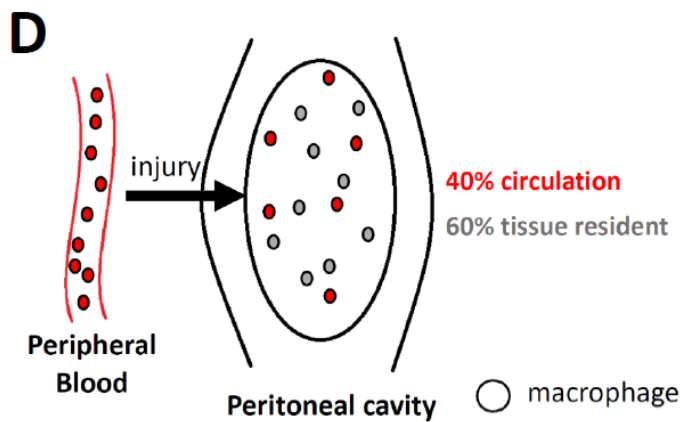
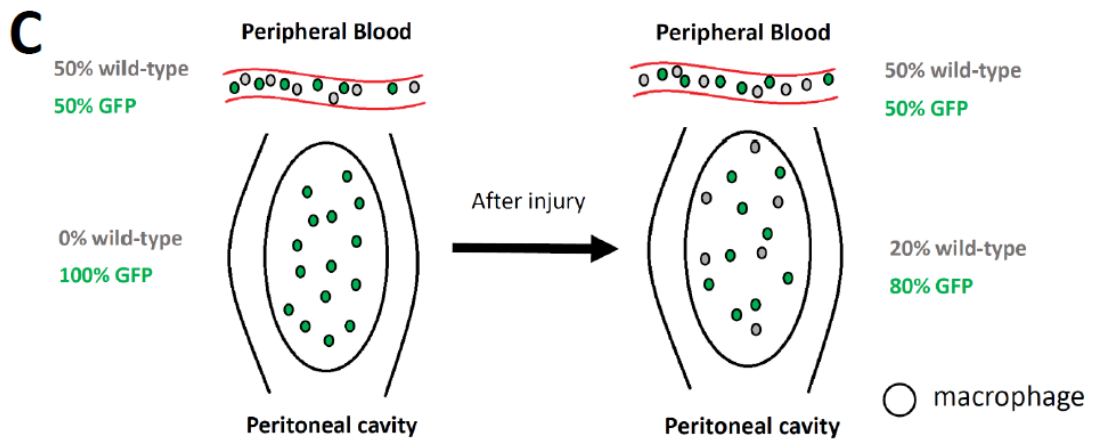
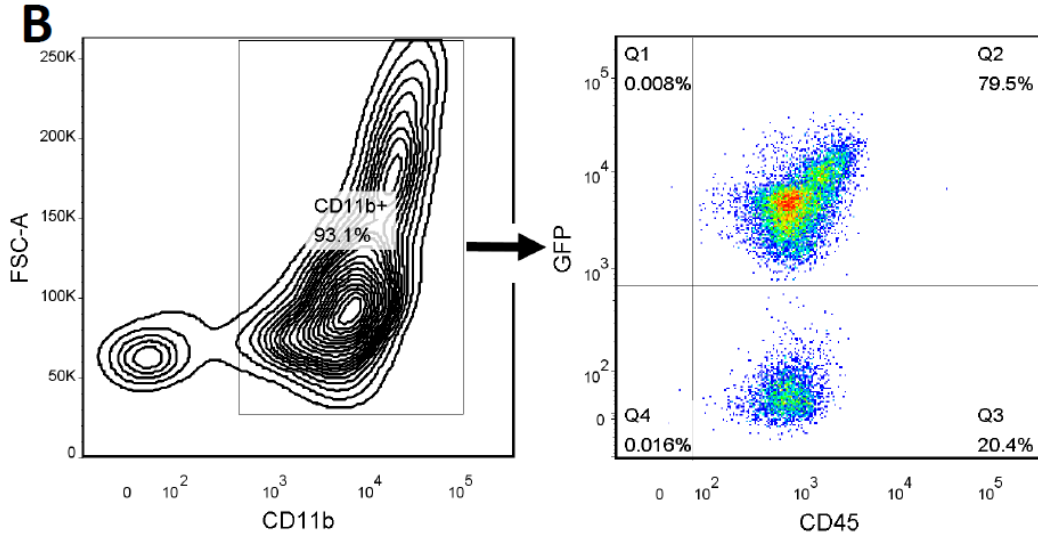
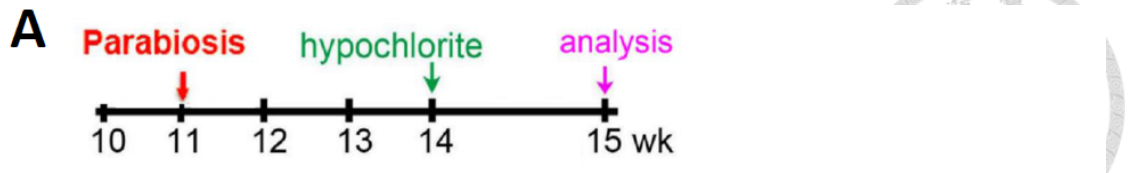
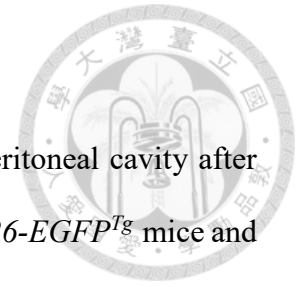
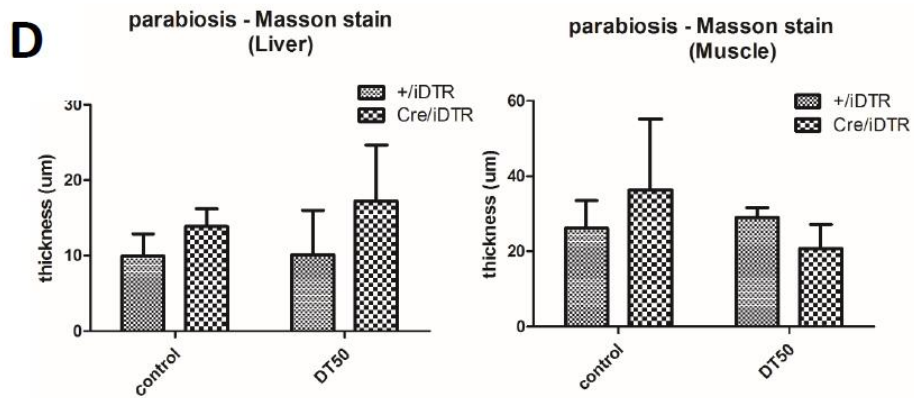
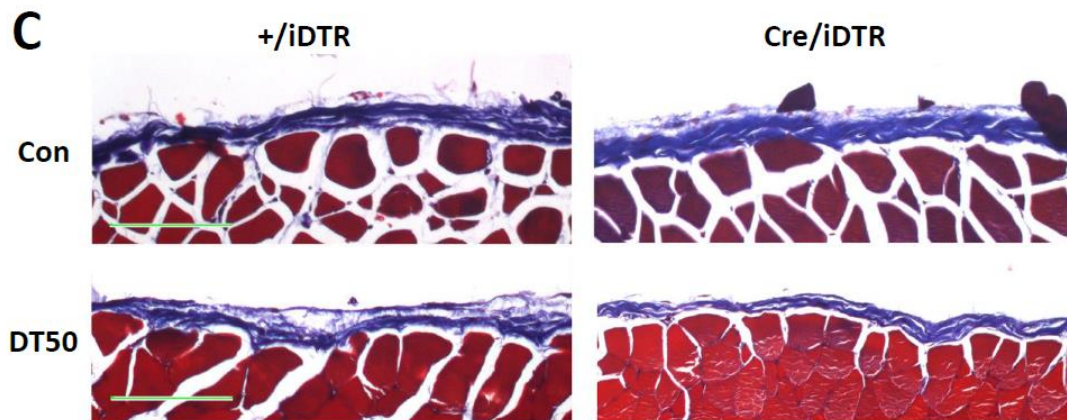
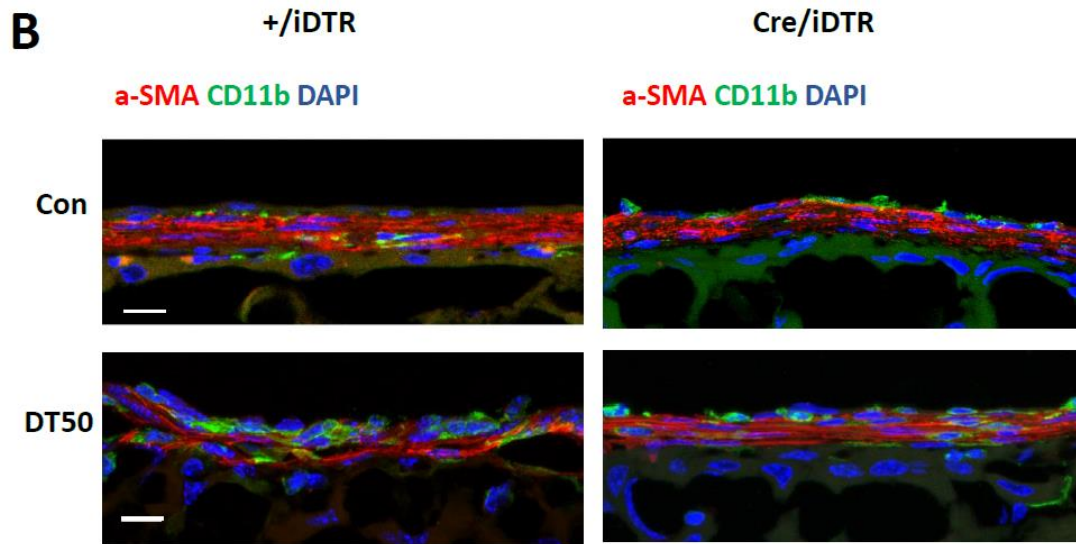
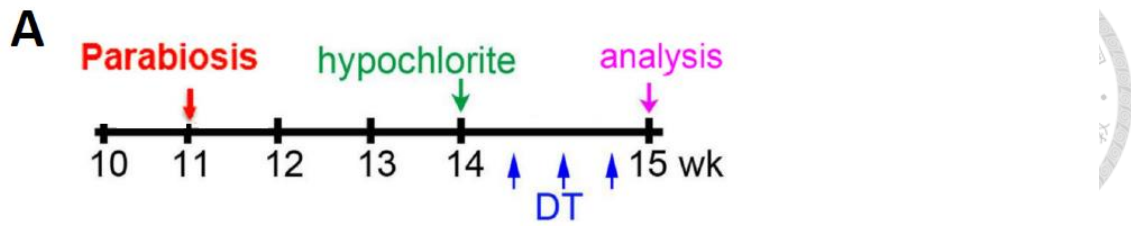


Figure 7

Circulating monocyte-derived macrophages recruited to peritoneal cavity after injury. (A) Experimental schema for parabiont mice of *Rs26-EGFP^{Tg}* mice and wild type (WT) *C57BL/6* mice after hypochlorite peritoneal injury. Peritoneal cavity cells were analyzed by flow cytometry 7 days after hypochlorite injury. (B) 20.4% were GFP⁻ cells and 79.5% were GFP⁺ cells in CD11b positive population in *Rs26-EGFP^{Tg}* mice. (C, D) Schema for 40% of circulating monocyte-derived macrophages recruit to peritoneal cavity after injury since GFP⁻ cells took up 50% in peripheral blood in parabiont.





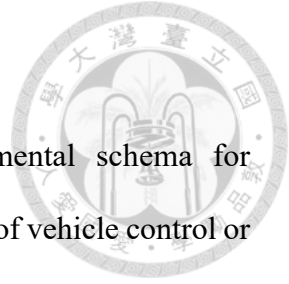
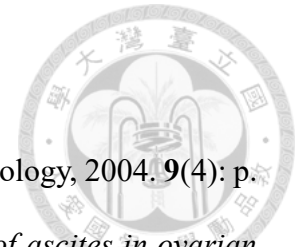


Figure 8

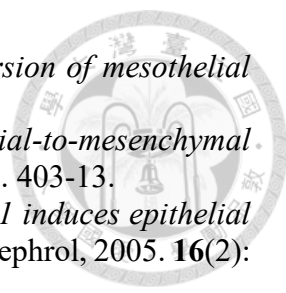
Macrophage ablation in parabiosis model. (A) Experimental schema for hypochlorite peritoneal injury and intraperitoneal injections of vehicle control or DT every other day from day 2 after peritoneal injury in parabiont mice of *Csf1r-Cre/Esr1^{Tg};Rs26^{iDTR/+}* (Cre/iDTR) and littermate control without Cre (+/iDTR). Analyses were performed on the peritoneal covering of liver 7 days after hypochlorite injury. (B) Immunofluorescence staining of α SMA and CD11b in control and DT group. The results showed that many CD11b positive cells accumulated in fibrosis area. (C) Masson's trichrome staining demonstrated that fibrosis severity of control and DT group was not different in the peritoneum overlying abdominal muscle wall. (D) Bar graphs showed the thickness of peritoneal membrane covering the surface of livers and muscle walls in injured peritoneum with control or DT injection. DAPI, 4',6-diamidino-2-phenylindole. Bar = 20 μ m (in B) and 100 μ m (in C). Original magnification, x630 (in B). Original magnification, x400 (in C).

REFERENCE



1. Mutsaers, S.E., et al., *Pathogenesis of pleural fibrosis*. *Respirology*, 2004. **9**(4): p. 428-40.
2. Kipps, E., D.S. Tan, and S.B. Kaye, *Meeting the challenge of ascites in ovarian cancer: new avenues for therapy and research*. *Nat Rev Cancer*, 2013. **13**(4): p. 273-82.
3. Mutsaers, S.E., *Mesothelial cells: their structure, function and role in serosal repair*. *Respirology*, 2002. **7**(3): p. 171-91.
4. Fukata, H., *Electron microscopic study on normal rat peritoneal mesothelium and its change in absorption of particulate iron dextran complex*. *Acta Pathol Jpn*, 1963. **13**: p. 309-25.
5. Davies, S.J., *Peritoneal solute transport and inflammation*. *Am J Kidney Dis*, 2014. **64**(6): p. 978-86.
6. Yao, V., et al., *Peritoneal mesothelial cells produce cytokines in a murine model of peritonitis*. *Surg Infect (Larchmt)*, 2004. **5**(3): p. 229-36.
7. Matte, I., et al., *Mesothelial cells interact with tumor cells for the formation of ovarian cancer multicellular spheroids in peritoneal effusions*. *Clin Exp Metastasis*, 2016.
8. Miao, Z.F., et al., *Tumor-associated mesothelial cells are negative prognostic factors in gastric cancer and promote peritoneal dissemination of adherent gastric cancer cells by chemotaxis*. *Tumour Biol*, 2014. **35**(6): p. 6105-11.
9. Devuyt, O., P.J. Margetts, and N. Topley, *The pathophysiology of the peritoneal membrane*. *J Am Soc Nephrol*, 2010. **21**(7): p. 1077-85.
10. Chen, Y.T., et al., *Lineage tracing reveals distinctive fates for mesothelial cells and submesothelial fibroblasts during peritoneal injury*. *J Am Soc Nephrol*, 2014. **25**(12): p. 2847-58.
11. Grassmann, A., et al., *ESRD patients in 2004: global overview of patient numbers, treatment modalities and associated trends*. *Nephrol Dial Transplant*, 2005. **20**(12): p. 2587-93.
12. Czyzewski, L., et al., *Assessment of health-related quality of life of patients after kidney transplantation in comparison with hemodialysis and peritoneal dialysis*. *Ann Transplant*, 2014. **19**: p. 576-85.
13. Liu, Y., et al., *Transition of mesothelial cell to fibroblast in peritoneal dialysis: EMT, stem cell or bystander?* *Perit Dial Int*, 2015. **35**(1): p. 14-25.
14. Shiao, C.C., et al., *Seven-year follow-up of peritoneal dialysis patients in Taiwan*. *Perit Dial Int*, 2009. **29**(4): p. 450-7.
15. Margetts, P.J. and K.S. Brimble, *Peritoneal dialysis, membranes and beyond*. *Curr Opin Nephrol Hypertens*, 2006. **15**(6): p. 571-6.
16. Fielding, C.A., et al., *Interleukin-6 signaling drives fibrosis in unresolved inflammation*. *Immunity*, 2014. **40**(1): p. 40-50.
17. Krediet, R.T. and D.G. Struijk, *Peritoneal changes in patients on long-term peritoneal dialysis*. *Nat Rev Nephrol*, 2013. **9**(7): p. 419-29.
18. Aroeira, L.S., et al., *Epithelial to mesenchymal transition and peritoneal membrane failure in peritoneal dialysis patients: pathologic significance and potential therapeutic interventions*. *J Am Soc Nephrol*, 2007. **18**(7): p. 2004-13.
19. Habib, S.M., et al., *Management of encapsulating peritoneal sclerosis: a*

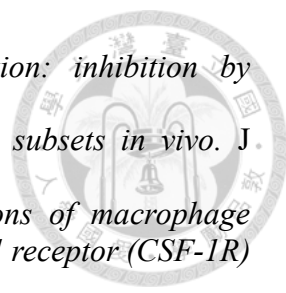
- guideline on optimal and uniform treatment. *Neth J Med*, 2011. **69**(11): p. 500-7.
20. Schilte, M.N., et al., *Factors contributing to peritoneal tissue remodeling in peritoneal dialysis*. *Perit Dial Int*, 2009. **29**(6): p. 605-17.
 21. Honda, K., et al., *Impact of uremia, diabetes, and peritoneal dialysis itself on the pathogenesis of peritoneal sclerosis: a quantitative study of peritoneal membrane morphology*. *Clin J Am Soc Nephrol*, 2008. **3**(3): p. 720-8.
 22. Padwal, M. and P.J. Margetts, *Experimental systems to study the origin of the myofibroblast in peritoneal fibrosis*. *Kidney Res Clin Pract*, 2016. **35**(3): p. 133-41.
 23. Yung, S. and T.M. Chan, *Intrinsic cells: mesothelial cells -- central players in regulating inflammation and resolution*. *Perit Dial Int*, 2009. **29 Suppl 2**: p. S21-7.
 24. Yamaguchi, N., et al., *Newly Developed Neutralized pH Icodextrin Dialysis Fluid: Nonclinical Evaluation*. *Artif Organs*, 2016. **40**(8): p. E158-66.
 25. Honda, K., et al., *Accumulation of advanced glycation end products in the peritoneal vasculature of continuous ambulatory peritoneal dialysis patients with low ultra-filtration*. *Nephrol Dial Transplant*, 1999. **14**(6): p. 1541-9.
 26. Combet, S., et al., *Vascular proliferation and enhanced expression of endothelial nitric oxide synthase in human peritoneum exposed to long-term peritoneal dialysis*. *J Am Soc Nephrol*, 2000. **11**(4): p. 717-28.
 27. Augustine, T., et al., *Encapsulating peritoneal sclerosis: clinical significance and implications*. *Nephron Clin Pract*, 2009. **111**(2): p. c149-54; discussion c154.
 28. Moinuddin, Z., et al., *Encapsulating peritoneal sclerosis-a rare but devastating peritoneal disease*. *Front Physiol*, 2014. **5**: p. 470.
 29. Park, S.H., Y.L. Kim, and B. Lindholm, *Experimental encapsulating peritoneal sclerosis models: pathogenesis and treatment*. *Perit Dial Int*, 2008. **28 Suppl 5**: p. S21-8.
 30. Mori, Y., et al., *A case of a dialysis patient with sclerosing peritonitis successfully treated with corticosteroid therapy alone*. *Am J Kidney Dis*, 1997. **30**(2): p. 275-8.
 31. Strippoli, R., et al., *Molecular Mechanisms Underlying Peritoneal EMT and Fibrosis*. *Stem Cells Int*, 2016. **2016**: p. 3543678.
 32. Holmdahl, L., et al., *Overproduction of transforming growth factor-beta1 (TGF-beta1) is associated with adhesion formation and peritoneal fibrinolytic impairment*. *Surgery*, 2001. **129**(5): p. 626-32.
 33. Tomura, S., et al., *Fibrinogen, coagulation factor VII, tissue plasminogen activator, plasminogen activator inhibitor-1, and lipid as cardiovascular risk factors in chronic hemodialysis and continuous ambulatory peritoneal dialysis patients*. *Am J Kidney Dis*, 1996. **27**(6): p. 848-54.
 34. Savagner, P., *Leaving the neighborhood: molecular mechanisms involved during epithelial-mesenchymal transition*. *Bioessays*, 2001. **23**(10): p. 912-23.
 35. Piek, E., et al., *TGF-(beta) type I receptor/ALK-5 and Smad proteins mediate epithelial to mesenchymal transdifferentiation in NMuMG breast epithelial cells*. *J Cell Sci*, 1999. **112 (Pt 24)**: p. 4557-68.
 36. Fan, J.M., et al., *Transforming growth factor-beta regulates tubular epithelial-myofibroblast transdifferentiation in vitro*. *Kidney Int*, 1999. **56**(4): p. 1455-67.
 37. Iwano, M., et al., *Evidence that fibroblasts derive from epithelium during tissue fibrosis*. *J Clin Invest*, 2002. **110**(3): p. 341-50.

- 
38. Yang, A.H., J.Y. Chen, and J.K. Lin, *Myofibroblastic conversion of mesothelial cells*. *Kidney Int*, 2003. **63**(4): p. 1530-9.
39. Yanez-Mo, M., et al., *Peritoneal dialysis and epithelial-to-mesenchymal transition of mesothelial cells*. *N Engl J Med*, 2003. **348**(5): p. 403-13.
40. Margetts, P.J., et al., *Transient overexpression of TGF- β 1 induces epithelial mesenchymal transition in the rodent peritoneum*. *J Am Soc Nephrol*, 2005. **16**(2): p. 425-36.
41. Aguilera, A., et al., *Epithelial to mesenchymal transition as a triggering factor of peritoneal membrane fibrosis and angiogenesis in peritoneal dialysis patients*. *Curr Opin Investig Drugs*, 2005. **6**(3): p. 262-8.
42. Hung, K.Y., et al., *Pentoxifylline modulates intracellular signalling of TGF- β in cultured human peritoneal mesothelial cells: implications for prevention of encapsulating peritoneal sclerosis*. *Nephrol Dial Transplant*, 2003. **18**(4): p. 670-6.
43. Mortier, S., A.S. De Vriese, and N. Lameire, *Recent concepts in the molecular biology of the peritoneal membrane - implications for more biocompatible dialysis solutions*. *Blood Purif*, 2003. **21**(1): p. 14-23.
44. Mortier, S., et al., *Effects of conventional and new peritoneal dialysis fluids on leukocyte recruitment in the rat peritoneal membrane*. *J Am Soc Nephrol*, 2003. **14**(5): p. 1296-306.
45. Devuyt, O., N. Topley, and J.D. Williams, *Morphological and functional changes in the dialysed peritoneal cavity: impact of more biocompatible solutions*. *Nephrol Dial Transplant*, 2002. **17 Suppl 3**: p. 12-5.
46. Davies, S.J., et al., *Determinants of peritoneal membrane function over time*. *Semin Nephrol*, 2011. **31**(2): p. 172-82.
47. Cho, Y., C.M. Hawley, and D.W. Johnson, *Clinical causes of inflammation in peritoneal dialysis patients*. *Int J Nephrol*, 2014. **2014**: p. 909373.
48. Lambie, M., et al., *Independent effects of systemic and peritoneal inflammation on peritoneal dialysis survival*. *J Am Soc Nephrol*, 2013. **24**(12): p. 2071-80.
49. Lambie, M.R., et al., *Peritoneal inflammation precedes encapsulating peritoneal sclerosis: results from the GLOBAL Fluid Study*. *Nephrol Dial Transplant*, 2016. **31**(3): p. 480-6.
50. Gerber, S.A., et al., *Preferential attachment of peritoneal tumor metastases to omental immune aggregates and possible role of a unique vascular microenvironment in metastatic survival and growth*. *Am J Pathol*, 2006. **169**(5): p. 1739-52.
51. Hurst, S.M., et al., *Il-6 and its soluble receptor orchestrate a temporal switch in the pattern of leukocyte recruitment seen during acute inflammation*. *Immunity*, 2001. **14**(6): p. 705-14.
52. Masunaga, Y., et al., *Ascites from patients with encapsulating peritoneal sclerosis augments NIH/3T3 fibroblast proliferation*. *Ther Apher Dial*, 2003. **7**(5): p. 486-93.
53. McLoughlin, R.M., et al., *Interplay between IFN- γ and IL-6 signaling governs neutrophil trafficking and apoptosis during acute inflammation*. *J Clin Invest*, 2003. **112**(4): p. 598-607.
54. Mozaffarian, A., et al., *Mechanisms of oncostatin M-induced pulmonary inflammation and fibrosis*. *J Immunol*, 2008. **181**(10): p. 7243-53.
55. Margetts, P.J., et al., *Inflammatory cytokines, angiogenesis, and fibrosis in the rat*

- peritoneum*. Am J Pathol, 2002. **160**(6): p. 2285-94.
56. Tekstra, J., et al., *Identification of the major chemokines that regulate cell influxes in peritoneal dialysis patients*. J Am Soc Nephrol, 1996. **7**(11): p. 2379-84.
57. Haslinger, B., et al., *Hyaluronan fragments induce the synthesis of MCP-1 and IL-8 in cultured human peritoneal mesothelial cells*. Cell Tissue Res, 2001. **305**(1): p. 79-86.
58. Breborowicz, A., et al., *Synthesis of hyaluronic acid by human peritoneal mesothelial cells: effect of cytokines and dialysate*. Perit Dial Int, 1996. **16**(4): p. 374-8.
59. Ha, H., et al., *Effects of conventional and new peritoneal dialysis solutions on human peritoneal mesothelial cell viability and proliferation*. Perit Dial Int, 2000. **20 Suppl 5**: p. S10-8.
60. Margetts, P.J., et al., *Gene transfer of transforming growth factor-beta1 to the rat peritoneum: effects on membrane function*. J Am Soc Nephrol, 2001. **12**(10): p. 2029-39.
61. Kawai, T. and S. Akira, *The role of pattern-recognition receptors in innate immunity: update on Toll-like receptors*. Nat Immunol, 2010. **11**(5): p. 373-84.
62. Colmont, C.S., et al., *Human peritoneal mesothelial cells respond to bacterial ligands through a specific subset of Toll-like receptors*. Nephrol Dial Transplant, 2011. **26**(12): p. 4079-90.
63. Kawasaki, T. and T. Kawai, *Toll-like receptor signaling pathways*. Front Immunol, 2014. **5**: p. 461.
64. Raby, A.C., et al., *Toll-Like Receptors 2 and 4 Are Potential Therapeutic Targets in Peritoneal Dialysis-Associated Fibrosis*. J Am Soc Nephrol, 2016.
65. Wang, H.H. and C.Y. Lin, *Interleukin-12 and -18 levels in peritoneal dialysate effluent correlate with the outcome of peritonitis in patients undergoing peritoneal dialysis: implications for the Type I/Type II T-cell immune response*. Am J Kidney Dis, 2005. **46**(2): p. 328-38.
66. Wang, H.H., T.Y. Lee, and C.Y. Lin, *Kinetics and involvement of interleukin-17 in the outcome of peritonitis in nondiabetic patients undergoing peritoneal dialysis*. J Chin Med Assoc, 2011. **74**(1): p. 11-5.
67. Mi, S., et al., *Blocking IL-17A promotes the resolution of pulmonary inflammation and fibrosis via TGF-beta1-dependent and -independent mechanisms*. J Immunol, 2011. **187**(6): p. 3003-14.
68. Rodrigues-Diez, R., et al., *IL-17A is a novel player in dialysis-induced peritoneal damage*. Kidney Int, 2014. **86**(2): p. 303-15.
69. Clark, R.B., et al., *The nuclear receptor PPAR gamma and immunoregulation: PPAR gamma mediates inhibition of helper T cell responses*. J Immunol, 2000. **164**(3): p. 1364-71.
70. Sandoval, P., et al., *PPAR-gamma agonist rosiglitazone protects peritoneal membrane from dialysis fluid-induced damage*. Lab Invest, 2010. **90**(10): p. 1517-32.
71. Zweers, M.M., et al., *Ultrastructure of basement membranes of peritoneal capillaries in a chronic peritoneal infusion model in the rat*. Nephrol Dial Transplant, 2001. **16**(3): p. 651-4.
72. Beelen, R.H., et al., *Rat models in peritoneal dialysis*. Nephrol Dial Transplant, 2001. **16**(3): p. 672-4.
73. Gonzalez-Mateo, G.T., et al., *Chronic exposure of mouse peritoneum to peritoneal*

- dialysis fluid: structural and functional alterations of the peritoneal membrane.* Perit Dial Int, 2009. **29**(2): p. 227-30.
74. Wang, J., et al., *The role of peritoneal alternatively activated macrophages in the process of peritoneal fibrosis related to peritoneal dialysis.* Int J Mol Sci, 2013. **14**(5): p. 10369-82.
75. Zareie, M., et al., *Peritoneal dialysis fluid-induced changes of the peritoneal membrane are reversible after peritoneal rest in rats.* Nephrol Dial Transplant, 2005. **20**(1): p. 189-93.
76. Kato, H., et al., *Atrial natriuretic peptide ameliorates peritoneal fibrosis in rat peritonitis model.* Nephrol Dial Transplant, 2012. **27**(2): p. 526-36.
77. Biswas, S.K. and A. Mantovani, *Macrophage plasticity and interaction with lymphocyte subsets: cancer as a paradigm.* Nat Immunol, 2010. **11**(10): p. 889-96.
78. van Furth, R., et al., *The mononuclear phagocyte system: a new classification of macrophages, monocytes, and their precursor cells.* Bull World Health Organ, 1972. **46**(6): p. 845-52.
79. Ginhoux, F., et al., *Fate mapping analysis reveals that adult microglia derive from primitive macrophages.* Science, 2010. **330**(6005): p. 841-5.
80. Schulz, C., et al., *A lineage of myeloid cells independent of Myb and hematopoietic stem cells.* Science, 2012. **336**(6077): p. 86-90.
81. Bain, C.C., et al., *Resident and pro-inflammatory macrophages in the colon represent alternative context-dependent fates of the same Ly6Chi monocyte precursors.* Mucosal Immunol, 2013. **6**(3): p. 498-510.
82. Tamoutounour, S., et al., *Origins and functional specialization of macrophages and of conventional and monocyte-derived dendritic cells in mouse skin.* Immunity, 2013. **39**(5): p. 925-38.
83. Gentek, R., K. Molawi, and M.H. Sieweke, *Tissue macrophage identity and self-renewal.* Immunol Rev, 2014. **262**(1): p. 56-73.
84. Lin, S.L., et al., *Macrophage Wnt7b is critical for kidney repair and regeneration.* Proc Natl Acad Sci U S A, 2010. **107**(9): p. 4194-9.
85. Wynn, T.A., A. Chawla, and J.W. Pollard, *Macrophage biology in development, homeostasis and disease.* Nature, 2013. **496**(7446): p. 445-55.
86. Lin, S.L., et al., *Bone marrow Ly6Chigh monocytes are selectively recruited to injured kidney and differentiate into functionally distinct populations.* J Immunol, 2009. **183**(10): p. 6733-43.
87. Braga, T.T., J.S. Agudelo, and N.O. Camara, *Macrophages During the Fibrotic Process: M2 as Friend and Foe.* Front Immunol, 2015. **6**: p. 602.
88. Sica, A. and A. Mantovani, *Macrophage plasticity and polarization: in vivo veritas.* J Clin Invest, 2012. **122**(3): p. 787-95.
89. Ghosn, E.E., et al., *Two physically, functionally, and developmentally distinct peritoneal macrophage subsets.* Proc Natl Acad Sci U S A, 2010. **107**(6): p. 2568-73.
90. Davies, L.C., et al., *Tissue-resident macrophages.* Nat Immunol, 2013. **14**(10): p. 986-95.
91. Okabe, Y. and R. Medzhitov, *Tissue-specific signals control reversible program of localization and functional polarization of macrophages.* Cell, 2014. **157**(4): p. 832-44.
92. Gautier, E.L., et al., *Gata6 regulates aspartoacylase expression in resident*

- peritoneal macrophages and controls their survival. J Exp Med, 2014. 211(8): p. 1525-31.*
93. Accarias, S., et al., *Single-cell analysis reveals new subset markers of murine peritoneal macrophages and highlights macrophage dynamics upon Staphylococcus aureus peritonitis. Innate Immun, 2016. 22(5): p. 382-92.*
 94. Wynn, T.A. and L. Barron, *Macrophages: master regulators of inflammation and fibrosis. Semin Liver Dis, 2010. 30(3): p. 245-57.*
 95. Duffield, J.S., et al., *Selective depletion of macrophages reveals distinct, opposing roles during liver injury and repair. J Clin Invest, 2005. 115(1): p. 56-65.*
 96. Wynn, T.A. and T.R. Ramalingam, *Mechanisms of fibrosis: therapeutic translation for fibrotic disease. Nat Med, 2012. 18(7): p. 1028-40.*
 97. Mosser, D.M. and J.P. Edwards, *Exploring the full spectrum of macrophage activation. Nat Rev Immunol, 2008. 8(12): p. 958-69.*
 98. Murray, P.J. and T.A. Wynn, *Protective and pathogenic functions of macrophage subsets. Nat Rev Immunol, 2011. 11(11): p. 723-37.*
 99. Greenfield, L., et al., *Nucleotide sequence of the structural gene for diphtheria toxin carried by corynebacteriophage beta. Proc Natl Acad Sci U S A, 1983. 80(22): p. 6853-7.*
 100. Honjo, T., Y. Nishizuka, and O. Hayaishi, *Diphtheria toxin-dependent adenosine diphosphate ribosylation of aminoacyl transferase II and inhibition of protein synthesis. J Biol Chem, 1968. 243(12): p. 3553-5.*
 101. Naglich, J.G., et al., *Expression cloning of a diphtheria toxin receptor: identity with a heparin-binding EGF-like growth factor precursor. Cell, 1992. 69(6): p. 1051-61.*
 102. Saito, M., et al., *Diphtheria toxin receptor-mediated conditional and targeted cell ablation in transgenic mice. Nat Biotechnol, 2001. 19(8): p. 746-50.*
 103. Buch, T., et al., *A Cre-inducible diphtheria toxin receptor mediates cell lineage ablation after toxin administration. Nat Methods, 2005. 2(6): p. 419-26.*
 104. Lin, S.L., et al., *Pericytes and perivascular fibroblasts are the primary source of collagen-producing cells in obstructive fibrosis of the kidney. Am J Pathol, 2008. 173(6): p. 1617-27.*
 105. Peters, S.O., et al., *Quantitative polymerase chain reaction-based assay with fluorogenic Y-chromosome specific probes to measure bone marrow chimerism in mice. J Immunol Methods, 2002. 260(1-2): p. 109-16.*
 106. Qian, B.Z., et al., *CCL2 recruits inflammatory monocytes to facilitate breast-tumour metastasis. Nature, 2011. 475(7355): p. 222-5.*
 107. Hashimoto, D., et al., *Tissue-resident macrophages self-maintain locally throughout adult life with minimal contribution from circulating monocytes. Immunity, 2013. 38(4): p. 792-804.*
 108. Wang, S., et al., *TGF-beta/Smad3 signalling regulates the transition of bone marrow-derived macrophages into myofibroblasts during tissue fibrosis. Oncotarget, 2016. 7(8): p. 8809-22.*
 109. Meng, X.M., et al., *Inflammatory macrophages can transdifferentiate into myofibroblasts during renal fibrosis. Cell Death Dis, 2016. 7(12): p. e2495.*
 110. Theiss, A.L., et al., *Tumor necrosis factor (TNF) alpha increases collagen accumulation and proliferation in intestinal myofibroblasts via TNF receptor 2. J Biol Chem, 2005. 280(43): p. 36099-109.*
 111. Porter, K.E., et al., *Tumor necrosis factor alpha induces human atrial*

- 
- myofibroblast proliferation, invasion and MMP-9 secretion: inhibition by simvastatin.* Cardiovasc Res, 2004. **64**(3): p. 507-15.
112. Loschko, J., et al., *Inducible targeting of cDCs and their subsets in vivo.* J. Immunol Methods, 2016. **434**: p. 32-8.
113. Hume, D.A. and K.P. MacDonald, *Therapeutic applications of macrophage colony-stimulating factor-1 (CSF-1) and antagonists of CSF-1 receptor (CSF-1R) signaling.* Blood, 2012. **119**(8): p. 1810-20.
114. MacDonald, K.P., et al., *An antibody against the colony-stimulating factor 1 receptor depletes the resident subset of monocytes and tissue- and tumor-associated macrophages but does not inhibit inflammation.* Blood, 2010. **116**(19): p. 3955-63.
115. Geissmann, F., et al., *Blood monocytes: distinct subsets, how they relate to dendritic cells, and their possible roles in the regulation of T-cell responses.* Immunol Cell Biol, 2008. **86**(5): p. 398-408.
116. Wei, S., et al., *Modulation of CSF-1-regulated post-natal development with anti-CSF-1 antibody.* Immunobiology, 2005. **210**(2-4): p. 109-19.
117. Cenci, S., et al., *M-CSF neutralization and egr-1 deficiency prevent ovariectomy-induced bone loss.* J Clin Invest, 2000. **105**(9): p. 1279-87.
118. Radi, Z.A., et al., *Increased serum enzyme levels associated with kupffer cell reduction with no signs of hepatic or skeletal muscle injury.* Am J Pathol, 2011. **179**(1): p. 240-7.